POLY (N-ISOPROPYLACRYLAMIDE) MICROGEL LATEXES

PREPARATION AND CHARACTERIZATION OF TEMPERATURE SENSITIVE POLY (N-ISOPROPYLACRYLAMIDE) MICROGEL LATEXES

By

WAYNE C. McPHEE, B.A.Sc.

A Thesis
Submitted to the School of Graduate Studies
in Partial Fulfillment of the Requirements
for the Degree
Master of Engineering

McMaster University
September, 1991

Masters of Engineering (1991) McMaster University
(Chemical Engineering) Hamilton, Ontario

TITLE: Preparation and Characterization of Temperature Sensitive Poly (N-isopropylacrylamide) Microgel Latexes

AUTHOR: Wayne Charles McPhee, B.A.Sc. (University of Toronto)

SUPERVISOR: Professor R. H. Pelton

NUMBER OF PAGES: vi, 122

Abstract

Temperature sensitive microgel latexes of poly (N-isopropylacrylamide) cross-linked with N-N'methylene bisacrylamide (BA) were prepared and characterized by Dynamic Light Scattering, Titration and Electrophoresis. The study of gels, including temperature sensitive gels, is limited by the large size of traditional bulk gels which are slow to respond to changes and are difficult to measure. An alternative system, which may be easier to study, is a microgel latex which would constitute small particles of gel which would respond quickly to changes in their environment and could also be measured using colloidal measuring techniques like dynamic light scattering and particle electrophoresis

Monodisperse and stable microgel latex particles were prepared by reacting N-isopropylacrylamide (NIPAM) monomer with a cross-linking agent BA in water at 70°C with a surfactant (sodium dodecylsulfate) present. Latexes prepared without surfactant were polydisperse.

Characterization of the poly (NIPAM) particles by dynamic light scattering at several different temperatures showed that the particles go through a transition from a water swollen gel at low temperature to a shrunken gel with a low water content at high temperature. The transition occurs about 32°C. The degree of swelling of the poly (NIPAM) particles can be expressed by the Flory-Huggins Interaction parameter c and is dependent upon the level of cross-linking agent included.

Titration and electrophoresis results indicate that the particles contain about 0.39 Coulombs per gram of polymer of carboxylic and sulfuric charged end groups which are distributed throughout the particle.

Acknowledgements

I would like to thank my wife, Eileen, whose love and patience and hard work made it possible for this thesis to be completed.

Thanks to my family who supported me in my decision to pursue a Masters and have continued to support me through to it's completion.

I would like to thank Dr. Bob Pelton for the time and effort he put into the numerous discussions we had about this research project and the time that he spent going over and commenting on this thesis.

Table of Contents

1. Introduction **1**
2. Theoretical and Literature Search **4**
2.1 Acrylamide Polymerization 4
2.2 N-isopropylacrylamide Polymers 7
2.2.1 Monomer 7
2.2.2 Homopolymer 7
2.2.3 Macroscopic Gels 10
2.2.4 NIPAM Gel Particles 13
2.3 Homogenous Nucleation 14
2.4 Swelling of Gels 16
2.5 Dynamic Light Scattering 19
2.6 Titration of the Charge on a Latex Particle 25
2.7 Volume Fraction of Polymer in Swollen Gel Latex Particles 28
2.8 Particle Electrophoresis 31
2.8.1 Factors Which Affect the Electrophoretic Mobility 32
2.8.2 O'Brien and White's Solution 37
3. Experimental **39**
3.1 Polymerization 39
3.1.3 Apparatus 39
3.1.2 Materials 41
3.1.3 Safety Considerations 42
3.1.4 Reaction 43
3.2 Cleaning Latexes by Ultracentrifugation 45
3.3 Particle Sizing 46
3.4 Particle Water Content 48
3.5 Titration 49
3.5.1 Ion Exchange 49
3.5.2 Running Titrations 50
3.5.3 Mass of Latex Titrated 52
3.6 Electrophoresis 53

4. Results and Discussions **55**
4.1 Polymerization 55
4.2 Volume Fraction of Polymer in Poly (NIPAM) Latex Particles 59
4.3 Gel Swelling 63
4.3.1 Effect of Ionic Strength on Gel Swelling 64
4.3.2 Effect of Temperature on Gel Swelling 67
4.3.4 Effect of Cross-linking Density on Gel Swelling 70
4.4 Titrations of Poly (NIPAM) Latexes 72
4.5 Electrophoresis of Poly (NIPAM) Latexes 77
5. Conclusions **81**
6. Bibliography **82**
7. Appendix **86**
Appendix 1 86
Appendix 2 (Raw Data) 87
Appendix 3 (Sample Calculations) 95
Appendix 4 Experimental Procedure and Data Analysis for
Coulter DELSA 440 Electrophoresis 100
A4.1 Introduction to DELSA 440 100
A4.1.1 Coulter Apparatus 100
A4.1.2 Laser Doppler Velocimetry 102
A4.1.3 Electrophoretic Mobility 103
A4.1.4 Electro-osmosis 104
A4.2 Experimental Procedure (Supplementary to Delsa Manual) 107
A4.2.1 Sample Preparation 107
A4.2.2 Finding the Stationary Layer 107
A4.2.3 Running Samples 109
A4.2.3.1 Voltage Selection 109
A4.3 Data Analysis 112
A4.3.1 Distribution Analysis 112
A4.3.2 Correcting for Electro-osmotic Flow 114
A4.3.3 Correction for Imperfect Tuning 118
A4.3.4 Correction for Error in Finding the Middle of the Cell 119
A4.3.5 Averaging the Mobilities at the Four Angles 121

1 Introduction

This thesis is a report on an experimental project which had the objective of producing and characterizing latexes of temperature sensitive poly(N-isopropylacrylamide) [poly (NIPAM)] gel.

Poly (NIPAM) is one of the acrylamide based family of polymers which have been used extensively as, amongst others, floculating agents and filter aids due to the fact that the properties of the polymer can be engineered to fit each specific application (Volk and Friedrich, 1980; MacWilliams, 1973). Poly (NIPAM) is not of great interest commercially, but because of the temperature sensitivity that poly (NIPAM) displays it has been of interest in the research community. At low temperatures, poly (NIPAM) is soluble in water; but as the temperature of the solution is raised through a transition temperature (called the lower critical solution temperature, or LCST) the polymer becomes insoluble and phase separates (Heskins and Guillet, 1968)

Gels which are made by crosslinking poly (NIPAM) with a crosslinking agent also exhibit a similar temperature sensitivity. At low temperatures, in an aqueous environment, poly (NIPAM) gels will swell with water. As the temperature is raised through the transition temperature the poly (NIPAM) gel will release water and shrink in size. This phenomena is referred to as a volume phase transition (Tanaka Et al.,1985; Hirokawa and Tanaka, 1984).

Poly (NIPAM) homopolymers and gels have been studied by researchers interested in, amongst others, the solution properties of polymers (Kubota Et al., 1990; Chiantore Et al., 1979) in theories of gel swelling and in the denaturing of biological polymers (Fujishige Et al., 1987).

The studies of poly (NIPAM) gels have generally involved the study of cylindrical pieces of gel which were made by polymerizing NIPAM monomer with a crosslinker in a small test tube (Hirotsu Et al., 1987). Measurements of the size of the gel pieces in a solution can be made with a microscope. The gel pieces take a long time to reach an equilibrium volume after a change in their environment (ie. a change in the temperature or the solvent the pieces are in). To improve upon the response time, researchers (Tanaka Et al., 1985) made beads of poly (NIPAM) gel by suspending a water monomer mixture in paraffin oil and then polymerizing. These poly (NIPAM) gel beads were then measured by microscope.

To make poly (NIPAM) gel beads with an even faster response time, Pelton Et al. (1986) made latex dispersions of poly (NIPAM) gel. The work by Pelton Et al.(1986) investigated a series of latex recipes which resulted in stable latex particles. In another paper (Pelton Et al., 1989), a representative poly (NIPAM) gel latex was characterized by photon correlation spectroscopy and particle electrophoresis. This initial characterization laid a solid foundation for the further investigation of poly (NIPAM) gel latexes and possibly the development of a useful model system for the study of gel swelling and volume phase transition.

To further investigate the properties of poly (NIPAM) gel latexes, a series of latexes were produced and characterized. Polymerizations were performed in water with varying ratios of NIPAM monomer, crosslinking agent, initiator and in some cases small amounts of surfactant. The objective was to produce stable, monodisperse latexes with a particle size of less than 10^{-6}m (1μm) that exhibit temperature sensitive swelling characteristics.

The temperature sensitive swelling properties were investigated by measuring the size of the latex particles by dynamic light scattering (DLS) as a function of temperature.

DLS was also performed on poly(NIPAM) gel latexes in ionic solutions to investigate the effects of charged groups on the swelling properties of the latexes. The number, type and position of these charged groups was investigated using titrations of the latex and particle electrophoresis.

2 Theoretical and Literature Search

2.1 Acrylamide Polymerization

Poly (acrylamide) and similar polymers and co-polymers (including poly (N-isopropylacrylamide) [poly (NIPAM)]) are used extensively in industry because they are soluble in water and can be used as flocculents in aqueous colloid systems. A table of some of the industrial uses of acrylamide polymers is presented in Figure 2.1.

Industry	**Uses**
Water Treatment	Concentration and treatment of sewage Water Clarification
Pulp and Paper	Flocculent for fibers and pigments Improved water drainage from paper White water clarification
Mining	Mine waste water treatment Flocculent to settle and concentrate suspended particles
Also Cement manufacture, Oil recovery, Gel electrophoresis, Gelled explosives	

Figure 2.1 Industrial Uses of Poly (acrylamide)

The properties of acrylamide have been researched extensively and many summaries have been published (Thomas and Wang, 1985; Volk and Friedrich, 1980; MacWilliams, 1973). Some relevant information from these reviews, which might be helpful in future discussions about NIPAM, have been included in this section.

Acrylamide is a vinyl monomer which polymerizes through the double bond (see Figure 2.2) to around 20,000 to 300,000 units, which means that typical molecular weights are between 1.4 million and 21 million. The polymerization follows the vinyl polymerization steps of initiation, propagation, chain transfer, and termination. The molecular weights for poly(acrylamide) are high because the ratio of the propagation rate constant to termination rate constant is high [$(k_p/k_t)^{1/2} = 4.2$ at 25°C]. As well, the amount of chain transfer to monomer is low. The only chain transfer which appears to be at all significant is transfer to initiator (K_2SO_4).

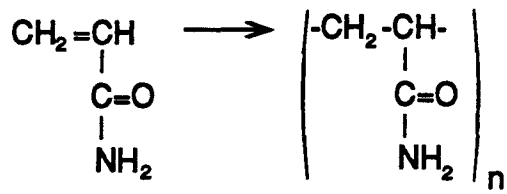

Figure 2.2 Acrylamide Polymerization

Gels of acrylamide can be made by copolymerizing acrylamide with a crosslinking agent like N-N'-methylene bisacrylamide (BA). It is necessary to use a crosslinking agent because acrylamide polymers do not usually branch. Some branches do form during reactions above 67°C when radicals attack the polymer backbone.

Poly (acrylamide) can also undergo hydrolysis of the amide group to form ionic polymers (Figure 2.3). The hydrolysis is catalyzed by either acidic or basic conditions.

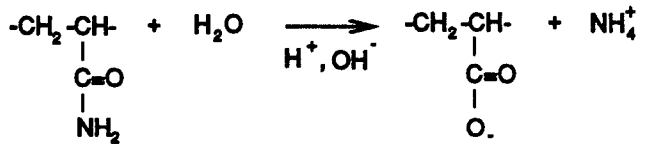

Figure 2.3 Hydrolysis of poly (acrylamide)

2.2 N-isopropylacrylamide Polymers

2.2.1 Monomer

N-isopropylacrylamide (NIPAM) is a vinyl monomer which, like acrylamide, will react through the double bond. NIPAM (shown in Figure 2.4) is soluble in most polar solvents. The solubility of NIPAM in water decreases as the temperature is raised (MacWilliams, 1973), which is the reverse to what happens in most chemicals.

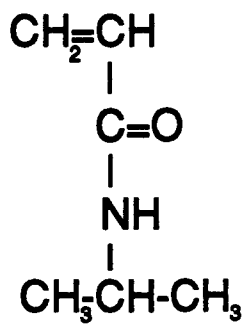

Figure 2.4 N-isopropylacrylamide (NIPAM)

2.2.2 Homopolymer

NIPAM monomer undergoes free radical polymerization to form a linear polymer (as shown in figure 2.5). Poly (NIPAM) homopolymer only dissolves in solvents which are capable of forming hydrogen bonds. In water, poly (NIPAM) will dissolve at low temperatures but at high temperatures the dissolved chains will collapse to form globules. This transition occurs at a temperature known as the lower critical solution temperature

(LCST). The LCST of poly (NIPAM) in pure water is about 31°C (Heskins and Guillet, 1968).

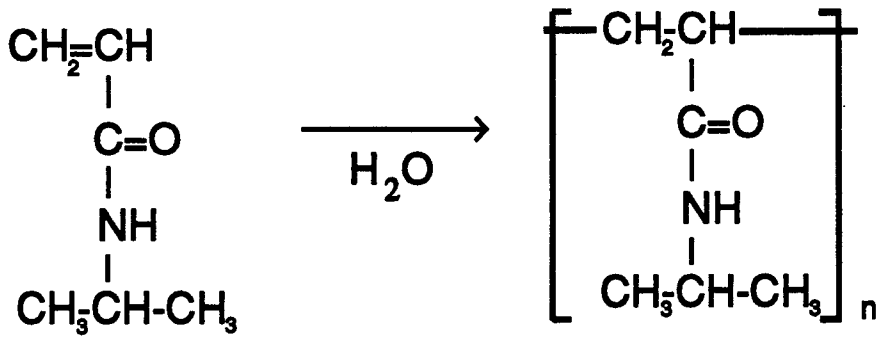

Figure 2.5 Polymerization of poly (NIPAM) homopolymer

One possible explanation for the existance of an LCST was presented by Heskins and Guillet (1968) as a combination of a decrease in the hydrogen bonding energy of water as the temperature is increased, and an increase of the entropy gained by the water when it is released by the polymer as it collapses.

At low temperature, a poly (NIPAM) chain is extended into solution because of the high energy of hydrogen bonds which develop between water molecules and the carbonyl amine groups on the NIPAM molecule. The extension of the polymer chain also exposes some of the propyl groups. Water forms a shell around the exposed propyl groups and causes a decrease in the entropy of the water molecules in the shell.

When the temperature is raised, the energy of the hydrogen bonds decreases and the entropy lost by water molecules forming a shell around the propyl group increases. At a certain temperature the Gibbs free energy (dG=dH-TdS) of a two phase globule system will become more negative than a single phase polymer solution, so the chains

will spontaneously collapse into phase separated globules. The water shell around the propyl groups will leave and the propyl groups will form into hydrophobic regions. There will be little room for water, so the amount of hydrogen bonding will decrease.

Chiantore et al. (1979, 1982) used intrinsic viscosity measurements to find the configuration of poly (NIPAM) homopolymers. They found that the chains were random coils at low temperature and then, as the temperature was raised above the LCST, the chains collapsed into globules.

Poly (NIPAM) homopolymers have been tested by examining the properties of the polymer-water system at temperatures above and below the LCST. The experimental techniques used to do this have included turbidity, static and dynamic light scattering, (Fujishige et al., 1989; Kubota et al., 1990) and intrinsic viscosity (Fujishige, 1987). An example of the results obtained by static and dynamic light scattering is shown in Figure 2.6.

Other studies of poly (NIPAM) show that the homopolymer has a glass transition temperature of 407°C (Chiantore et al., 1982) and a molar volume of 101.2 cm^3/mol (Zana, 1980).

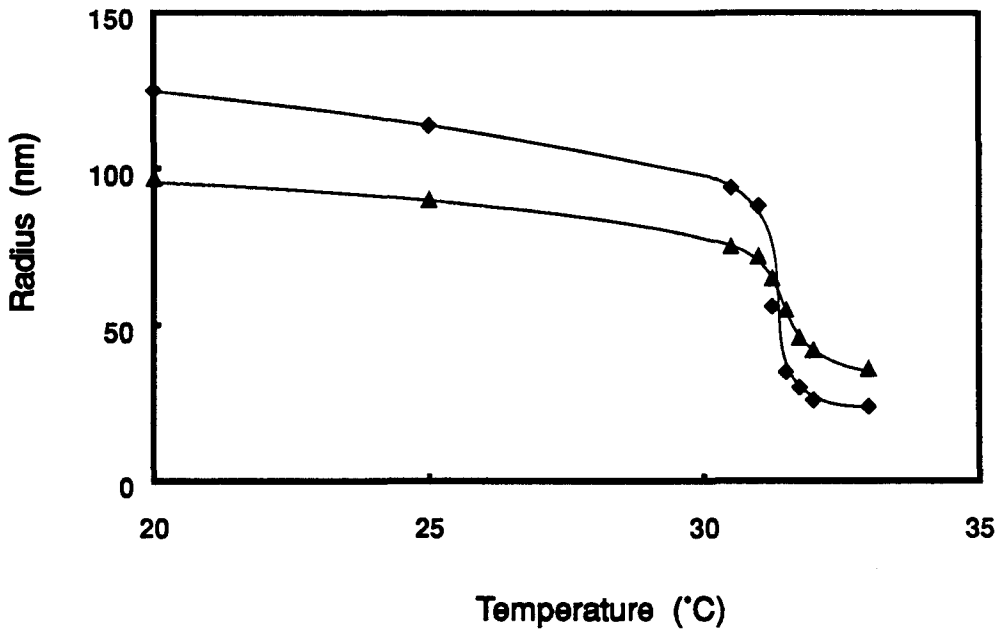

Figure 2.6 Static light scattering (diamonds) and dynamic light scattering (triangles) of NIPAM homopolymer heated through the LCST (data replotted from Fujishige et al., 1989)

2.2.3 Macroscopic Gels

Interest in poly (NIPAM) gels has arisen from a need for temperature sensitive gels and as a means of studying the behaviour of poly (NIPAM) homopolymer. The size of a piece of macroscopic gel can be measured using a microscope, which simplifies the experimental procedures necessary for analysing a poly (NIPAM) system. The macroscopic gels are usually made in test tubes with a diameter of approximately 1 millimeter (Hirotsu et al., 1987).

Poly (NIPAM) macroscopic gels in an aqueous environment display properties similar to those of the linear homopolymer. Instead of changing from an extended chain to a globule as the temperature is raised through the critical temperature, the gels will swell with water below the critical temperature. When the temperature is raised, they will expel some of the water and shrink in size.

Gels of poly (NIPAM) are prepared by dissolving NIPAM monomer in water along with a crosslinking agent, usually N-N'methylene bisacrylamide (BA) and reacting in a test tube (See Figure 2.7). The gels are then removed from the test tube, washed and placed in a solution which is accurately temperature controlled. A microscope is used to measure the size of the gels so the swelling of the gel can be found.

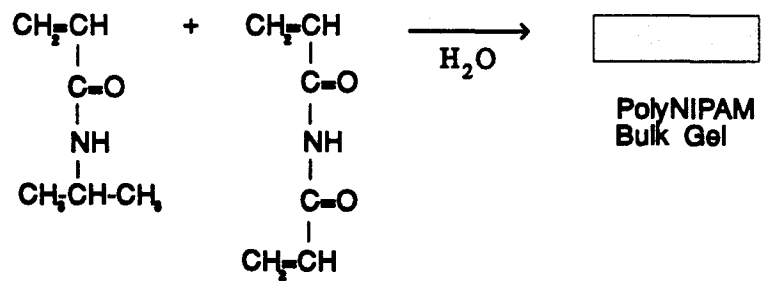

Figure 2.7 Preparation of macroscopic poly (NIPAM) gels

The temperature-dependent swelling of these poly (NIPAM) gels has been tested in water (Hirokawa and Tanaka, 1984) and in water-methanol mixtures (Hirotsu, 1988; Hirotsu, 1987). The Flory interaction parameter (χ), which is an expression of the polymer-solvent interaction, was found to have both an entropy and enthalpy component. These two components express the explanation for the LCST given by Heskins and Guillet (1968), which combined an enthalpy effect (the decrease in the energy of hydro-

gen bonding as the temperature was raised) and an entropy effect (the change in entropy as the water molecules left the shell around the propyl group).

Hirotsu (1987) expressed the Flory parameter (χ) as a sum of enthalpic and entropic contributions,

$$\chi = 1/k\ (\ dh/T + ds\ ) \qquad \textbf{(2.1)}$$

where k is Boltzmann's constant, T is the temperature in Kelvin, dh is a constant expressing the enthalpic contribution, and ds is a constant for the entropic contribution. Hirotsu found that dh and ds are constant below the critical temperature but change significantly above the critical temperature.

The properties of ionic poly (NIPAM) gels, made by the reaction of NIPAM and BA with an ionic comonomer, like sodium acrylate or acrylic acid, were also studied. The swelling of these ionized gels was found to be dependent on pH and ionic strength of the solution, as well as the temperature (Amiya et al., 1987; Hirotsu etal. 1987). In another study (Hirotsu, 1985), the swelling of ionic poly (NIPAM) gels was found to change under the influence of an applied electric field. The minimum level of ionic groups in these gels studied for electric field effects was about 1 part by weight of ionic monomer to 99 parts NIPAM monomer.

2.2.4 NIPAM Gel Particles

The study of poly (NIPAM) gels is hindered by the large size of the bulk gels that take a long time to adjust to changes in the conditions of the solution. In an attempt to improve this, researchers (Hirotsu, 1985; Hirokawa et al., 1985; Tanaka etal., 1985) made beads of gel by suspending drops of a monomer solution in paraffin oil and reacting. The resulting gel beads were between 50 and 300 micrometers in size and could be studied by detecting size changes with a microscope, which is similar to the techniques used for bulk gels.

A further improvement was made by Pelton et al. (1986, 1989) who made colloidal dispersions of poly (NIPAM) gels in water. The procedure for polymerization followed the same technique as employed by Goodwin et al. (1978) for the surfactant-free polymerization of polystyrene.

The colloidal nature of these particles allowed them to be studied by the same techniques used to study colloidal particles. Several techniques used by Pelton et al. included transmission electron microscopy, turbidity, electrophoresis, and dynamic light scattering. The colloidal particles showed the same swelling and shrinking characteristics at the critical temperature as both the homopolymer and the macroscopic gels. The small colloidal particles (< 1 μm) provide very quick response to changes in the solution conditions and allow the researcher to use several detection techniques as opposed to the one (a microscope) which can be used on a bulk gel.

2.3 Homogenous Nucleation

The model of homogenous nucleation was developed by Freeney Et al. (1987) to describe the surfactant-free latex polymerizations of styrene which were performed by Goodwin Et al. (1978,1979). A description of the physical concepts, which were used by Freeney Et al. to develop the mathematical model, will be presented here, as the same concepts apply to the production of NIPAM microgel latexes.

A stable dispersion of polymer particles can be produced in a polar solvent, without the presence of an emulsifier, if the decomposition of the initiator provides an ionic end group to the polymer molecules and the polymer molecules are insoluble in the solvent. The polymer will form a separate phase which, if stabilized, will result in stable particles dispersed in the solvent. In the system used by Goodwin Et al.(1978, 1979), styrene monomer was dissolved in water and initiated with an ionic initiator. The particles formed were polystyrene stabilized with the ionic end groups from the initiator located at the end of the polymer chains.

Initiator molecules decompose when heated and form radical molecules which react with monomers in solution to form monomer radicals. These propagate and then terminate to form polymer chains. As the polymer radical grows in solution it will reach a length where it becomes insoluble. At this point the polymer will form a spherical particle in order to reduce its surface area. The core of this particle is hydrophobic and so the charge groups from the surfactant move to the surface of the particle and provide a degree of stabilization.

The particles grow by two mechanisms, further polymerization and coagulation with other particles. Polymerization continues as the monomer which is in the particle is initiated by a radical. This radical can be either an initiator radical or an oligomer radical, where the polymer has not reached a sufficient length to become insoluble. Termination occurs if another radical enters the particle and terminates the existing radical.

Coagulation occurs when particles which are not large enough to be stable collide as a result of Brownian motion. Particle collision is not enough to bring about coagulation. The force of collision must be high enough to overcome the charge stabilization on the surface of the particle. The particles become stable when the surface charge is high enough that the forces generated by Brownian motion are not high enough to overcome the repulsive charge barrier.

The homogenous nucleation model may also apply to the polymerization of NIPAM in water above the critical temperature and initiated by an ionic initiator. NIPAM polymer chains are insoluble above the critical temperature, which is one of the characteristics of a homogenous nucleation system.

2.4 Swelling of Gels

Gels swell in solvent to an equilibrium volume which is related to the solubility of the polymer molecules and the amount of crosslinking or network structure which exists. Flory (1953) expressed the change in free energy of a pure gel in a pure solvent as a summation of the free energy of mixing of the polymer chains (ΔF_M) and the elastic free energy of the gel network stretching when swollen(ΔF_{el}). That is,

$$\Delta F = \Delta F_M + \Delta F_{el}. \qquad (2.2)$$

Flory used equations for the free energy of mixing of linear polymers to express ΔF_M and equations for the rubber elasticity of deformed polymer solids to express ΔF_{el}. Flory then differentiated the free energy equation to solve for the chemical potential.

An equilibrium volume (or maximum swelling condition) occurs when the chemical potential of the system is zero. By solving the chemical potential equation for a chemical potential of zero, Flory found a balance between the mixing potential and the elastic stretching energy. The equation, as expressed by Vold and Vold (1983) is,

$$\frac{V_1 \upsilon_e}{V_0}\left(\phi_2^{1/3} - \phi_2/2 \right) = -[\, \ln(1-\phi_2) + \phi_2 + \chi \phi_2^2 \,] \qquad (2.3)$$

where V_1 is the molar volume of the solvent the gel is swollen with (in m^3/mol), υ_e is the effective number of polymer chains (in moles), V_0 is the volume of polymer in the gel

(in m^3), ϕ_2 is the volume fraction of polymer and χ is the Flory interaction parameter.

The effective number of polymer chains, υ_e, is the number of segments of polymer chains which are in between two crosslinks. Any end of a polymer chain which is only held in the network by one point is not included in the count of the effective number. Flory found that the effective number of polymer, υ_e, could be expressed as

$$\upsilon_e = \mu_j \phi / 2$$

where μ_j is the number of junctions (or crosslinks) in a gel system and ϕ is the functionality of the crosslinks (Vold and Vold, 1983). For a poly (NIPAM) gel crosslinked with BA, a divinyl monomer, the functionality, ϕ, is 2. This means that υ_e is equal to μ_j which is the number of crosslinks or the number of moles of BA which have formed crosslinks in the gel.

The terms for the effective number of polymer chains and the volume of polymer can be combined to give the effective number of polymer chains per volume of polymer which is equal to the number of crosslinks per volume of polymer, μ_j / V_0. If the assumption is made that all BA molecules form crosslinks then μ_j / V_0 can be expressed in terms of the mass ratio of BA monomer to NIPAM monomer in the gel polymerization recipe, W_{NIPAM} / W_{BA}

$$\frac{\upsilon_e}{V_0} = \frac{\rho_p}{MW_{BA}} \times \frac{1}{1 + \frac{W_{NIPAM}}{W_{BA}}} \qquad (2.4)$$

where ρ_p is the density of NIPAM homopolymer and MW_{BA} is the molecular weight of BA.

The volume fraction of polymer, ϕ_2, in a poly (NIPAM) gel latex can be expressed as the volume of polymer in a latex particle, V_p, over the swollen volume of the particle at a given temperature, V_T; that is $\phi_2 = V_P/V_T$.

The Flory gel swelling equation for a poly (NIPAM) gel crosslinked with BA can be expressed as

$$\frac{V_1 \rho_P}{MW_{BA}} \times \frac{1}{1 + \frac{W_{NIPAM}}{W_{BA}}} \times \left(\left(\frac{V_P}{V_T} \right)^{1/3} - \frac{V_P}{2V_T} \right) = \left[\ln\left(1 - \frac{V_P}{V_T}\right) + \frac{V_P}{V_T} + \chi \left(\frac{V_P}{V_T} \right)^2 \right] \quad (2.5)$$

which can be applied to poly (NIPAM) gel system when the temperature is below the critical temperature and the gel is swollen.

2.5 Dynamic Light Scattering

Dynamic Light Scattering (DLS) is a technique for determining the size of particles suspended in a liquid medium. It is also called Quasi-Elastic Light Scattering, Time Dependent Light Scattering and Photon Correlation Spectroscopy.

Colloidal particles in a liquid medium will move randomly because of Brownian motion. The amount of motion will depend on the viscosity of the medium and the shape and size of the particle (Barth, 1984). DLS uses laser light scattering to detect particle movement, which can be related to particle size by specifying a shape.

The detection of particle movement is done by analysing the laser light which is scattered from the particle at an angle of 90° (as shown in Figure 2.8). The laser light is scattered from more than one particle so a correlation of all of the scattered light must be done. The light from two particles will interfere constructively if the light waves are in phase or destructively if the waves are out of phase.

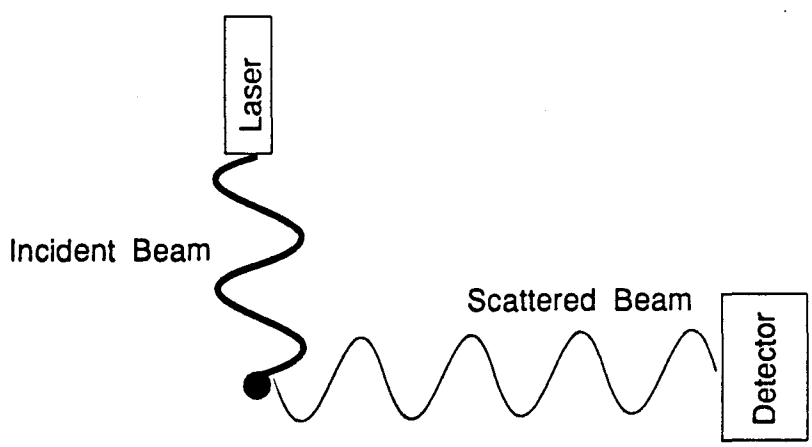

Figure 2.8 Light scattering from a particle at a right angle

The phase of the light wave is dependent on the positions of the particles. For example, particles which are separated by a distance equal to a multiple of the wavelength of the laser light will scatter light which is in phase. Particles which are a multiple of the wavelength plus one half the wavelength apart will scatter light which is out of phase (see Figure 2.9). Light which interferes constructively will have a higher amplitude and therefore a higher intensity than light which has destructively interfered.

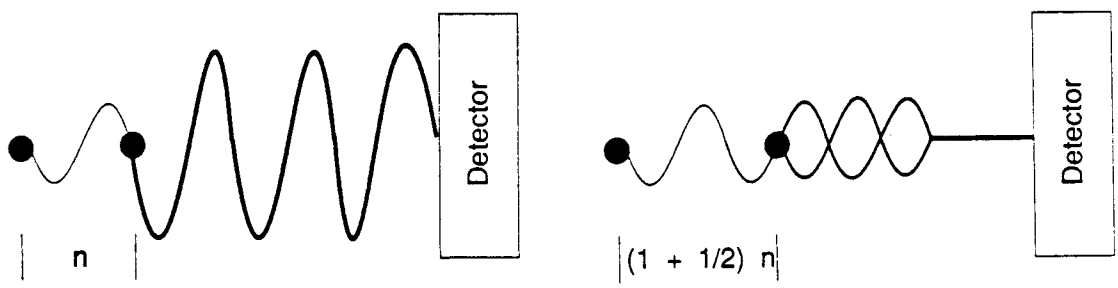

Figure 2.9 Interference of light scattered from two particles a) at distance n and b) at distance (1+1/2)n

As the particles undergo Brownian motion, the distances between the particles and the detector changes and so the intensity of the light which reaches the detector changes. The fluctuations in the intensity of the light can be related to the amount of Brownian motion and then to the size of the particle. For a small particle the Brownian motion will be high and so the fluctuations will be rapid. A comparison of small, medium and large particles is shown in Figure 2.10

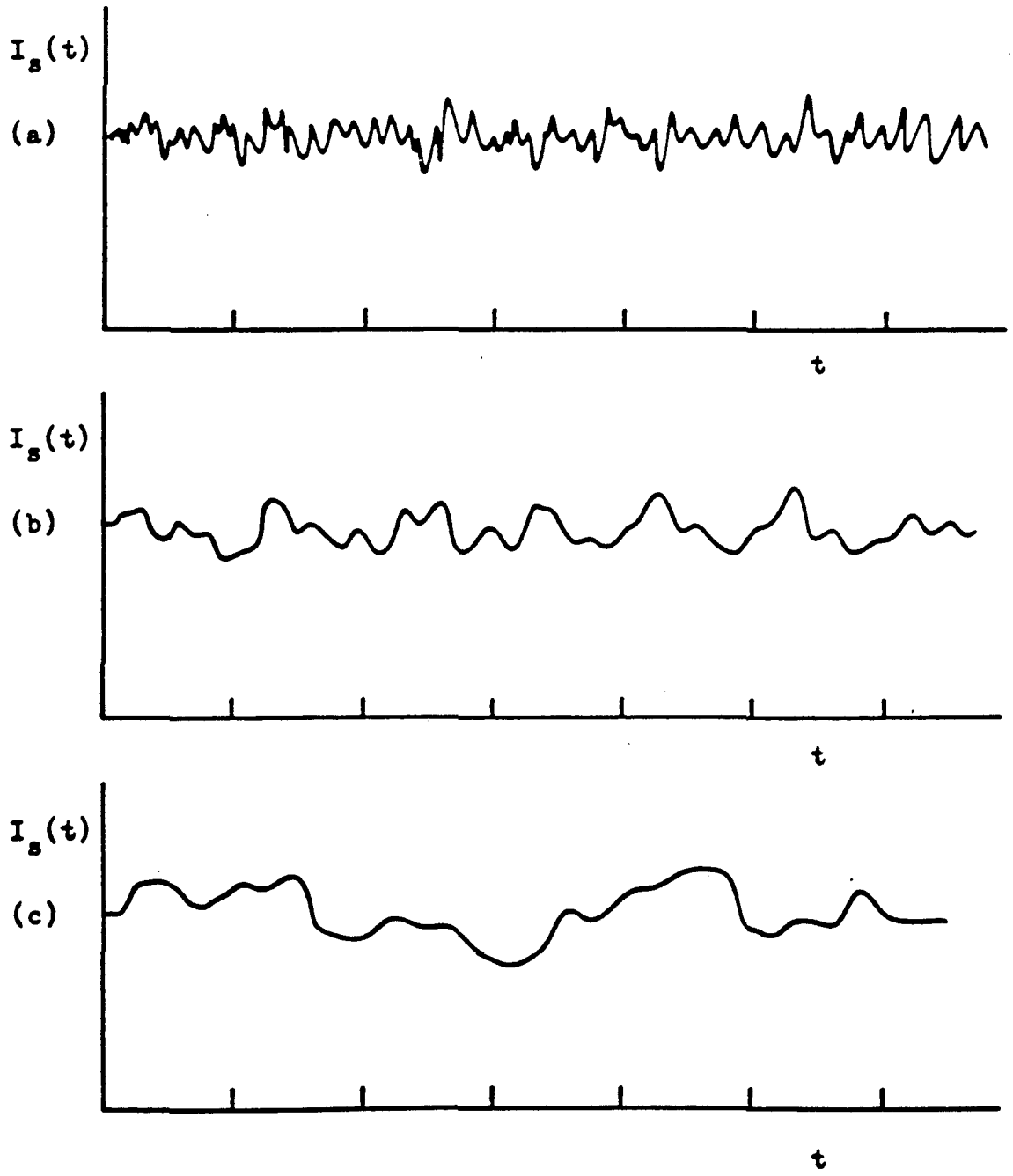

Figure 2.10 Comparison of intensity fluctuations from a) small size particles, b) medium size particles and c) large particles (from the NICOMP manual)

The frequency of the intensity fluctuations can be related to the diffusion coefficient of the particles which, if the particles are assumed to be spheres, can be converted to hydrodynamic radius of the particle using the Stokes-Einstein relationship

$$D = kT / 6\pi\eta R \qquad (2.6)$$

where D is the diffusion coefficient, k is Boltzmann's constant, T is the temperature, η is the viscosity of the solvent and R is the hydrodynamic radius of the particle.

The radius of all of the particles in a system are rarely all the same, so Laplace transforms can be used to solve the intensity fluctuations for a distribution of diffusion coefficients and a distribution of radii. The NICOMP system, which is used in this thesis, assumes the distribution is a Gaussian distribution, with a mean diameter and a standard deviation.

The initial form of the distribution is an intensity weighted distribution where the distribution of diameters are weighted by the intensity of the light which has a frequency fluctuation corresponding to each diameter. The intensity weighting requires no assumptions about the shape or properties of the particles but it has limited use. To be of more use, the distribution should be converted into a number or volume weighted distribution.

To convert from an intensity distribution to a number or volume distribution a relationship between the intensity of the light scattered by a particle and the volume of a particle must be established. For a particle with a diameter much smaller than the wavelength of the laser light, the relationship is based on the Rayleigh theory of scattering

where the intensity is related to the volume squared or the diameter to the power of six, $I \alpha D6$. Unfortunately, this simple relation only holds for particles with radii of less than one tenth the wavelength of the laser light (in the NICOMP $R< 50nm$).

For larger particles, the effect of intraparticle interference must be taken into consideration. In this case, light scattered from one part of a particle will interfere with light scattered from another part of the same particle. To convert them it is necessary to find the relative amount of light that is scattered from a particle as a function of the particle volume.

Mie scattering theory is used to relate the intensity of a large particle to the volume of the particle, but it requires some knowledge of the structure of the particle. The NICOMP contains two selections for the structure of the particle, a solid sphere and a hollow sphere (also called a vesicle). The structure of a swollen NIPAM gel particle does not fit under either of these structures.

David Nicoli (1990) suggested that applying Mie theory for a solid sphere to a swollen gel would overestimate the correction needed. The theory for a solid sphere is based on the assumption that light will be scattered by all of the volume of the particle. In a gel swollen by water only the fraction of the particle which is polymer will scatter light so the amount of intraparticle interference will be greatly reduced.

The Mie theory for a swollen sphere makes assumptions which do not apply to the case of swollen gel particles, so this method cannot be used to convert intensity weighted to volume weighted distributions. The derivation of a new method of conver-

sion would be difficult without further knowledge of the particle structure.

The value for the intensity weighted size of the particles is usually quite close to the volume weighted distribution for monodisperse solid spheres. For a case where the intraparticle interference is reduced, the real volume weighting should be close to the intensity weighted distribution. The intensity weighting could then be used as an approximation of the real volume weighted diameter of the particle.

2.6 Titration of the Charge on a Latex Particle

The amount of an acid or base in a solution is often found by titrating the solution with an acid or base of known concentration. Titration can also be used to find the number of charged groups on a latex particle. Latexes differ from free acids and bases because charged groups are bound to particles and are immobile. The two types of titrations that are commonly used to investigate the charge on latex particles are conductometric and potentiometric titrations.

Conductometric titrations are done by measuring the conductivity of a latex as a function of the acid and base added. The end points of the titration can be found by extrapolating the straight line segments to accurately find the inflection points in the conductivity curve. A strong acid will have one inflection point. The amount of base added between zero and the inflection point will be the amount of strong acid present. A weak acid will have two inflection points. The amount of acid added between the inflection points is the amount of weak acid present. In a system with both a strong and a weak acid present a condiometric titration curve will have two inflection points. The amount of base added between zero and the first inflection point is the amount of strong acid present and the the amount of base added between the first and second inflection points is the amount of weak acid present. The second inflection point also gives the total amount of acid present in the system.

Potentiometric titrations are done by measuring the pH of a latex as a function of the acid and base added. The end point of a potentiometric titration can be found at an

inflection point in the Ph curve. The inflection point is where the slope of the pH curve is at a maximum. This is true for both strong and weak acids. When both a strong and a weak acid are present, the amount of base added at the maximum of the pH curve is the total amount of acid present.

Usually in latex polymerizations there is more than one type of charge group present, which complicates the analysis. For instance, when persulphate is used as an initiator there can be sulphate groups, which are strong acid groups, and carboxyl groups, which are weak acid groups. The carboxyl groups are a result of hydrolysis of the carbon next to the sulphate group. In cases where both strong and weak acid groups are present it is helpful to have both conductometric and potentiometric titration curves to compare.

The charged groups on the latex particle surface which are being titrated must be put into an acid or base form before performing the titration. A charged group may be in a salt form which would not be detected by the titration. Ion exchange resins must be used to replace all the salt counter ions with hydrogen or hydroxyl counter ions.

Performing a titration is also complicated by impurities in the latex. According to Stenius Et al. (1983) and El Aasser (1983) the minimum level of impurities is 10 to 20 μmol/m3. The impurities can be carbon dioxide dissolved in the water, surfactant or other ions which might be on an unclean latex, or polyions which have desorbed from the ion exchange resin. Carbon dioxide can be controlled, but not totally removed, by flushing the latex with nitrogen and maintaining a nitrogen blanket during titration (El Aasser, 1983). If a latex is well cleaned before titrating, the levels of impurities from the polymerization should be insignificant. The polyions which will desorb from one ion exchange resin will be adsorbed by an opposite ion exchange resin. Using a mixed bed of

ion exchange resins, that is both a cationic resin and a anionic resin, will reduce the level of impurities. As well, Vanderhoff et al.(1970) found that fewer polyions leach from cleaned ion exchange resins.

2.7 Volume Fraction of Polymer in Swollen Gel Latex Particles

A common method for cleaning polymer latexes is by centrifuging the latex into a compact mass, decanting the supernate and then redispersing the latex in a clean solvent (El-Aasser, 1983; Vanderhoff, 1970). The centrifugation of latexes also lends itself to the investigation of the amount of water in a swollen gel latex. The volume of a compact mass of gel latex can be considered to be composed of three sections; the volume of the polymer in the particles; the volume of water in the particles and the interstitial volume of water in between the particles.

The volume fraction of polymer in a single particle can be found by finding the volume ratio of polymer to water in a centrifuged latex and then accounting for the interstitial volume between the particles. It may be possible to estimate the interstitial volume by making one of two simplifying assumptions. One assumption would be that the particles are deformed by the centrifugal force so that there is no interstitial volume. In this case the volume fraction of polymer in the particles could be written as:

$$\frac{V_P}{V_T} = \frac{V_P}{V_P + V_W} \qquad (2.7)$$

where V_P is the volume of polymer, V_W is the volume of water and V_T is the total volume.

The results from an experiment, where a gel latex was centrifuged to a compact mass and then dried, would include the mass of wet latex and the mass of dry polymer.

The volume of polymer would then be $V_p = M_p/\rho_p$ where M_p is the mass of the dry polymer and ρ_p is the density of the dry polymer. The volume of water would be $V_w = M_w/\rho_w$ where ρ_w is the density of water and M_w is the mass of water which is equal to the difference between the total mass and the mass of dry polymer or $M_w = M_T - M_P$. The equation for the volume of polymer in the latex particles, assuming that the volume of the poly (NIPAM) and the water are additive, can then be found as:

$$\frac{V_P}{V_T} = \frac{M_P/\rho_p}{(M_T - M_P)/\rho_w + M_P/\rho_p} \qquad (2.8)$$

A second simplifying assumption that can be made is that the particles are packed into some logical order by the centrifugation. The close packing of hard spheres results in a packing pattern which is called rhombohedral (Fayed and Otten, 1984) or hexagonal close packed. The ratio of interstitial volume to total volume, or the porosity (ε), of a rhombohedral packing arrangement has been found to be ε=0.2595 (Fayed and Otten, 1984; Linoya et al., 1984).

The volume fraction of polymer in the latex particles is once again;

$$\frac{V_P}{V_T} = \frac{V_P}{V_P + V_w} \qquad (2.7)$$

The volume of wet gel V_{Gel} is equal to the sum of the volume of polymer, the volume of water and the interstitial volume, V_I or $V_{Gel} = V_P + V_W + V_I$. The volume fraction of polymer then becomes:

$$\frac{V_P}{V_T} = \frac{V_P}{V_P + V_W + V_I} \qquad (2.9)$$

The interstital volume can be related to the total volume of the gel by the porosity, $V_I = \varepsilon V_{Gel}$. The volume fraction of polymer can then be expressed as a function of the volume of gel and the porosity;

$$\frac{V_P}{V_T} = \frac{V_P}{(1-\varepsilon)\, V_{GEL}} \qquad (2\text{-}10)$$

The results from an experiment would include the mass of dry polymer, M_p, and the mass of wet gel, M_{Gel}. The mass of wet gel less the mass of the dry polymer would give a value for the total mass of water in the gel. The volume fraction of polymer in the latex particles would then be:

$$\frac{V_P}{V_T} = \frac{1}{1-\varepsilon} \times \frac{M_P/\rho_P}{(M_{GEL} - M_P)/\rho_W + M_P/\rho_P} \qquad (2\text{-}11)$$

The reasonable estimate for the volume fraction of polymer in a particle can be found from experimental data if the correct simplifying assumption or the packing arrangment of the particles can be determined.

2.8 Particle Electrophoresis

A charged particle which is placed in an electric field will move with a velocity , U, where

$$U = m E, \qquad (2.12)$$

where E is the applied electric field and m is the electrophoretic mobility. Theoretical analysis has been done to relate the electrophoretic mobility of a particle to the shape and size of the particle and to the electrical potential at the shear plane of the particle. Many types of particles have been studied. The most common type of particle studied is solid spherical polymer particles (Eagland and Allen, 1977; Goff and Luner, 1984; Midmore and Hunter, 1988; O'Brien and White, 1978; Zukoski and Saville, 1985 and 1986). Liquid emulsions have also been studied (Ohshima Et al., 1982). Even non-spherical particles like cylinders and ellipses (Yoon and Kim, 1989) have been studied.

As well, researchers have studied spherical particles which do not have a single, discrete surface of charge but a layer of charge on the surface which has a finite thickness. This includes biological particles with charged membranes or proteins sticking out into solution (Donath and Putoshenko, 1979; Ohshima and Kondo, 1987) and bitumen particles which have high surface roughness (Chow and Takamura, 1988).

The goal of most researchers has been to relate the electrophoretic mobility to the amount of charge on the particle or the electrical potential of the surface of the particle. Traditionally, a relationship was developed which related the mobility of a particle to the electrical potential at the plane of shear of the particle.

A charged particle which is motionless in an electrolyte solution will have a electrical potential of zero because counter charges form in a layer around the particle which neutralizes the particle. When the particle is in motion, the movement of fluid past the particle will remove some of these counter charges and leave the particle with an electrical potential. This potential, at the plane of shear, is called the zeta potential (ζ).

2.8.1 Factors Which Affect the Electrophoretic Mobility

There are many factors which affect the electrophoretic mobility of a charged particle in an electric field. These factors can be broken down into properties of the electrical double layer around the particle, the solution the particle is in and the particle itself.

A charged particle which is motionless in an aqueous medium will appear to be neutral because a region of counter charges forms around the particle. This region is considered to composed of two layers of charge which are called the Stern layer and the diffuse layer. The stern layer is layer of concentrated charge right next to the particle surface and the diffuse layer extends out into the solution. The size of this double layer will have a strong effect on the mobility of the particle.

The size of the double layer is usually expressed by the Debye-Huckel length. The Debye Huckel derivation is based on the assumption that the double layer can be modelled as a capacitor and the distance between the capacitor plates is called the Debye Huckel length and given the symbol κ^{-1}.

The distance κ^{-1} can by found by deriving the equation for the electrical potential at a point at distance x from the surface of the particle. The potential is found to be (Hiemenz,)

$$\psi = \psi_o \exp(-\kappa x) \qquad (2.13)$$

where ψ is the potential at a distance x

ψ_o the surface potential

κ inverse Debye Huckel length ($1/\kappa^{-1}$).

The distance κ^{-1} then is the distance where the potential drops to 1/e of the surface potential. The actual length of the double layer is considered to be between $3\kappa^{-1}$ to $4\kappa^{-1}$, which is where the potential has dropped so low that it is negligible. In theory the potential and double layer extend to infinity.

The value of κ^{-1} is usually found using the Debye Huckel approximation, which holds for potential lower than 25 mV (Hiemenz, 1986). The inverse Debye Huckel length is;

$$\kappa = \left[\frac{e^2 \, Na \, \sum z_i M_i}{\varepsilon \, kT} \right] \qquad (2.14)$$

where e is the charge of an electron, Na is Avogadros Number, ε is the dielectric constant, k is boltzmann's constant, T is the temperature in Kelvin, z_i is the valence of the ith electrolyte and M_i is the molarity of the ith electrolyte.

The size of the double layer is dependent on the type of solvent used (which determines the dielectric constant), the type and concentration of electrolytes and the temperature of the system. The solvent is usually water so the dielectric constant will only depend on the temperature. The double layer will increase with increasing temperature. The size of the double layer is reduced by either an increase in the valency or the concentration of the electrolyte.

The effect that the size of the double layer has on the mobility of the particle can be simply understood by examining where the shear plane intercepts the potential curve (see figure 2.11. If the double layer extends a large distance into the solution (κ^{-1} is large) then, when the particle is moved, the shear of the fluid will remove a large amount of counter charge and leave the particle with a high total charge and therefore a high mobility. Alternatively, if the double layer is reduced, the shear will remove less counter charge and will leave the particle with less total charge and the particle will therefore have a lower mobility.

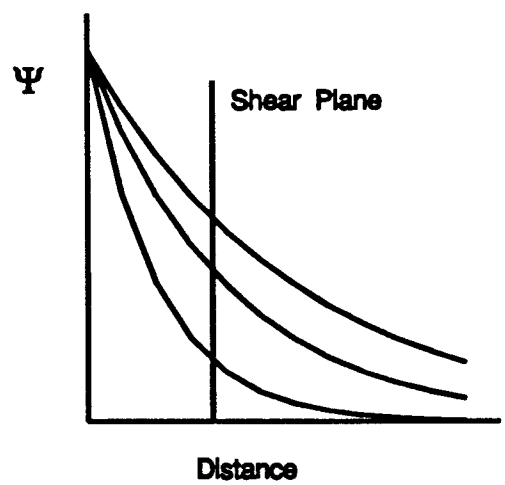

Figure 2.11 Electrical Potential for different values of κ showing the electrical potential at the plane of shear

This simple analysis is complicated by the movement of charge within the double layer and charge relaxation effects. Relaxation effects are a result of the counter ions removed by the shear of fluid tailing behind the particle. The counter ions are sheared off of the particle by fluid movement and move, in the opposite direction to the particle, along electric field lines. This will result in a counter ion cloud which will attract the particle towards it, retard the movement of the particle, and decrease the mobility of the particle.

Surface conductance also exists in the double layer so the double layer will be distorted by the movement of the particle. The double layer will not retain a uniform thickness all around the particle which will effect the mobility directly and by contributing to the relaxation effects.

The size of the double layer is determined by the conditions of the solution that the particle is in, but the solvent itself also has effect on the mobility of the particle. The force put on the particle by the electric field is opposed by a viscous drag force, which for a spherical particle, follows Stokes equation. The viscosity of the solution is dependent on the type of solvent and the temperature.

Properties of the particle which effect the electrophoretic mobility of the particle include the shape and size of the particle, the surface charge and the particle conductance. The drag of a spherical particle through a liquid medium is dependent on the size of the particle.

The surface charge on the particle has a large influence on the mobility. If two similar particles have different charges, the one with a higher charge should, in general, have a higher mobility. In some cases with high surface charge, the relaxation effects become significant and some researchers (Wiersema,Et al, 1966) predict that the mobility will reach a maximum at some surface charge and any increase in surface charge will decrease the mobility.

The conductance of the material which makes up the bulk of a particle is often considered to be important to the mobility of a particle. The disturbance of the electric field by the presence of the particle leads to the relaxation effects which were discussed above.

The first disturbance of the electric field to be analyzed was by Smoluchowski in 1921, who approximated that the electric field around a particle always would be uniform and parallel to the particle surface. It was found later that this was only true when the size of the particle was much larger than the size of the double layer. This is expressed as $\kappa a \ll 1$ where κ is the inverse Debye Huckel length and a is the radius of the particle. In this case the mobility (μ) is found to be,(Hiemenz, 1986)

$$\mu = \varepsilon \zeta / \eta \qquad (2.15)$$

where ε is the dielectric constant, ζ is the zeta potential and η is the viscosity of the solvent.

In the other extreme, Huckel used an approximation that the electric field was not disturbed by the particle. This approximation only holds when the double layer is much bigger than the particle or $\kappa a \gg 1$. In this case the mobility was found to be

(Hiemenz, 1986),

$$\mu = {}^{2}/_{3}\ \varepsilon\, \zeta/\eta \qquad (2.16)$$

It is generally accepted that these two approximations are valid at the extreme conditions specified and most mobility theories will approach the Smoluchowski and Huckel equations for the mobility at these extreme conditions.

In between these two extremes, there have been several attempts to relate the mobility to the zeta potential. Henry, in 1931, (as discussed in Hiemenz , 1986) developed equations for the mobility which depended on the conductance of the particle. More recently, O'Brien and White (1978) and Oshima Et al. (1984) developed a theory for the mobility which assumes that all the deformation of the electric field takes place because of the potential in the double layer and the potential on the surface of the particle.

2.8.2 O'Brien and White's Solution

Initially it was possible to solve analytically for relationships between the mobility and the zeta potential but as the theory became more complicated it was necessary to develop computer programs to solve the multiple differential equations involved. Wiersemal (1966) computed and published tables which related the reduced mobility to κa for various values of the reduced zeta potential.

The reduced mobility and zeta potential are dimensionless forms of the mobility and zeta potential. The reduced mobility is,

$$E = \frac{3\,\eta\varepsilon}{2\varepsilon kT}\,\mu \qquad (2.17)$$

where E is the reduced mobility, μ is the mobility and the other constants are as presented previously. The reduced zeta potential is,

$$y = \frac{\varepsilon}{kT} \zeta \qquad (2.18)$$

where y is the reduced zeta potential, ζ is the zeta potential.

More recently, O'Brien and White have made a computer program available for other researchers to compute the mobility, zeta potential and surface charge density for their specific system.

The theory developed by O'Brien and White (1978) is based on a force balance of the forces acting on the particle. The force trying to move the particle is the electric force produced by the electric field and the resisting forces are the viscous force and the retardation force produced by the counter ion cloud. They also found that the inertial forces of accelerating the particle were negligible for most normal colloid systems.

The theory shows that the properties of the colloidal particle and the choice of the electrostatic boundary conditions are not factors in the computation of the mobility. The mobility is a function of the surface charge of the particle, without any shear, but it is not dependent on the model for the electrostatic boundary layer. This means that it is possible to compute the mobility of a particle from the surface charge without making assumptions about the position of the shear plane or finding the zeta potential.

3 Experimental

3.1 Polymerization

Poly (NIPAM) gel latexes were produced by reacting NIPAM monomer with a crosslinking agent, above the critical temperature, in water, in a well stirred reaction flask.

3.1.1 Apparatus

The polymerization was performed in a one litre covered glass reaction flask. The flask was made air tight with a rubber O-ring and a circular clamp which was used to secure the cover on the flask. The cover had four sealable access ports which were used to add reagents to the system, provide an access port for a stirrer and to allow for a nitrogen atmosphere to be maintained above the reaction mixture (see Figure 3.1). The temperature of the reaction mixture was controlled by suspending the reaction flask in a water bath with temperature control. A nitrogen line was fed into the flask to purge the water and maintain a nitrogen atmosphere for the reaction. The nitrogen flow exitted through a condenser to prevent loss of water by evaporation. The reaction solution was stirred by a mechanical stirrer with a glass rod and a teflon blade.

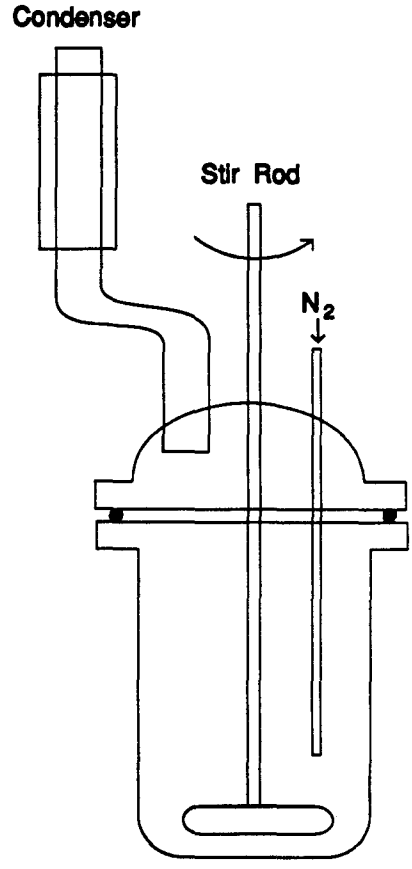

Figure 3.1 Reaction Flask

3.1.2 Materials

The ingredients used in the polymerization were two monomers N-isopropylacrylamide (NIPAM) and N-N'-methylene bisacrylamide (BA),a surfactant sodium dodecylsulphate (SDS), an initiator potassium persulphate (KPS) and ultrapure water from a Millipore water system. The SDS (Aldrich) and KPS (BDH, Analytical) were used as provided.

NIPAM (Kodak) was recrystallized to remove the inhibitor by the following procedure. NIPAM monomer was dissolved in toluene (Caledon, Reagent) at roughly 1 gram NIPAM to 1 mL toluene by heating the toluene to about 50°C. N-hexane (Caledon, Reagent), a non-solvent, was added at about 1 mL N-hexane per 2 mL toluene. If NIPAM did not crystallize, sodium sulphate (Fisher, Anhydrous) was added to the solution to absorb any water which might be present. To avoid later separation of the sodium sulphate from the NIPAM crystals, the sodium sulphate was placed in a piece of folded filter paper which was dipped into the toluene/n-hexane/NIPAM solution. After roughly ten minutes the filter paper was removed from the solution and the outside of the filter paper was rinsed with a little toluene to remove any NIPAM from the filter paper.

The solution was then put into a bucket of ice water and long white crystals, as described by MacWilliams (1973), were allowed to develop for several hours. The crystals were then filtered with a Buchner filter and were washed with n-hexane. The crystals were subsequently placed in a bottle and dried by gently blowing Nitrogen into the bottle for

about eight hours. When dry the NIPAM crystals were sealed in the bottle and stored in the dark at 5°C.

N-N'-methylene bisacrylamide (BA) was recrystallized from industrial grade BA. BA was dissolved in methanol (BDH, Analytical), at 1 gram per 10 mL methanol, by heating the methanol to about 50 °C. Some impurities did not dissolve in methanol and gave the solution a yellow colour. The impurities were filtered using a normal funnel and filter paper and washed with methanol to remove any BA. The clear filtrate was placed in ice water for several hours to allow the BA to crystallize. The crystals were filtered in a Buchner filter and washed with a small amount of cold methanol. The crystals were placed in a bottle and dried under nitrogen. The bottle was sealed and stored in the dark at 5 °C.

3.1.3 Safety Considerations

NIPAM and BA monomers are both toxic chemicals which must be handled with caution. All work performed on these monomers, including recrystallizations and reactions, was performed in a fume hood with the following safety precautions. When handling either of these chemicals a lab coat, safety glasses and two pairs of vinyl medical gloves was worn. If monomer crystals or a solution of monomer was spilled on to the gloves the outer poair was removed and replaced with a clean pair. The dirty contaminated gloves were placed in a solids disposal container in the fume hood. The lab coat worn was a disposable polyproylene coat which could be discarded in the solids disposal container if any monomer was spilled on the coat. Any other disposable objects which

came in contact with the monomers was also placed in the solids disposal container. Periodically the solid waste in the fume hood was sealed, labelled and disposed of at the facilities provided at McMaster University.

All glass ware which came in contact with either monomer was carefully washed with water before being removed from the fumehood. The wash water and any solvents which came in contact with the monomers was poured into solvent disposal bottles, labelled and disposed of at the facilities provided at McMaster University.

3.1.4 Reaction

The reaction vessel was washed with chromic acid and flushed with copious amounts of tap water followed by large amounts of Millipore water. The vessel was then placed in a water bath and the cover was clamped on. A rubber O-ring was placed between the kettle and the cover to insure a good seal. The vessel was held in place in the water bath by supports on the clamp.

The stirrer, nitrogen (Liquid Air, UHP) feed, and condenser were attached and the cooling water on the condenser was turned on. The stirrer was carefully alligned so that it would turn freely.

The flask was filled with 400 mL of Millipore water and the monomers and the surfactant were added. About 70 mL of Millipore water was used to wash off the weighing trays that were used to weigh the monomer crystals. The initiator, KPS, was dissolved in 30 mL of Millipore water .

After purging the system with nitrogen for 30 minutes, while stirring at 200 rpm, the initiator solution was added to the reaction flask and the reaction was allowed to proceed for four hours. The resulting latex was removed from the water and stored in a bottle at 5 °C to prevent bacterial growth.

3.2 Cleaning Latexes by Ultracentrifugation

The NIPAM latex, produced by the reaction described above, contains many impurities which were removed in order to study the latex. The impurities included any SDS used, unreacted initiator and polymer molecules which were not attached to the gel matrix (ie. sol fraction).

To remove the impurities the particles were ultracentrifuged in a (Beckman L7) Ultracentrifuge using a fixed angle rotor and 20mL polycarbonate tubes. The temperature of the centrifuge was set at 20 °C and the latex were centrifuged at 10,000 and 50,000 rpm depending on the density of the particles in the latex for one hour. The particles were ultracentrifuged into a compact mass of gel, the supernate was poured off and the particles were redispersed in Millipore water. This procedure was repeated four times to ensure that all of the impurities were removed. Appendix 1 contains data to show that four repetitions of this procedure were sufficient to get clean latexes.

3.3) Particle Sizing

The particle size of the NIPAM latexes was found using a NICOMP 370 submicron particle sizer (Pacific Scientific) which uses the technique of dynamic light scattering. Dilute samples of clean NIPAM latexes were prepared and the intensity weighted mean diameter of the particles was found by the following procedure.

Dilute samples were prepared by adding one or two drops of a clean NIPAM latex to 10mL solutions of either potassium chloride (KCl) or hydrogen chloride (HCl). Samples of the dilute latex solutions were put into small cuvettes and put into the NICOMP for analysis. Samples were left in the NICOMP for fifteen minutes so that the temperature could stabilize and then the analysis was started.

The NICOMP displays values for the mean diameter of the particle and the standard deviation of the particle size distribution. The mean diameter is found from the intensity weighted average of the particle sizes but it can be converted to the volume or number weighted distribution if desired. As discussed in the Section 2.5, poly (NIPAM) particles do not fit into the model for the theoretical conversion of the intensity weighted average to the volume or number weighted distribution so only the intensity weighted distribution and the standard deviation were recorded.

The NICOMP displays the diameter of the particles as a function of the time of operation so it is possible to determine when the diameter and standard deviation values

have stabilized. A printout of the particle size versus time was taken (see the example in Figure 3.2) when the diameter values and standard deviation had reached stable values.

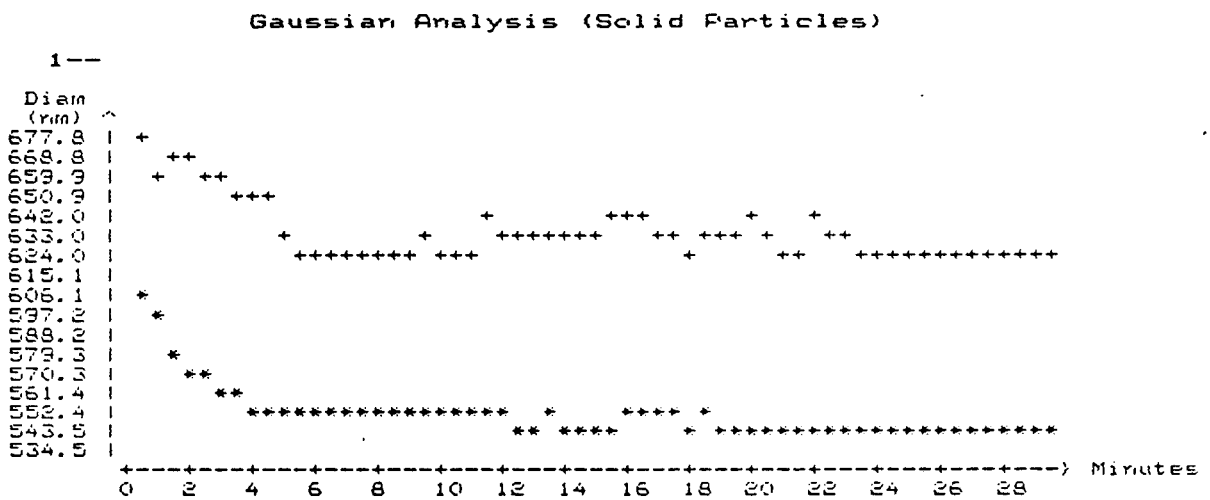

Figure 3.2 Printout from the NICOMP 370 Particle Sizer showing the time taken for the diameter values to stabilize (* is the intensity weighted average and + is the volume weighted average. The difference between the two values is an indication of the standard deviation)

3.4 Particle Water Content

The water content of the particles was found by ultracentrifuging the particles into a compact gel and then finding finding the water content of the gel, by drying. The ultracentrifuge tubes and settings were the same as those discussed in Section 3.2. The latex was spun down in the ultracentrifuge until it was a compact mass. The supernate was decanted and a portion of the gel was placed in a preweighed dish and weighed. The gel was dried in a vacuum oven, at around 40 °C, for four hours and then weighed again.

3.5 Titration

Titrations were performed to find the number of charged groups in a poly (NIPAM) latex. The latexes were first treated with a mixed bed ion exchange resin to convert all of the charged groups to their acid or base form. The latexes were then titrated and a sample of the latex was taken so that the mass of the latex titrated could be found.

3.5.1 Ion Exchange

The ion exchange resins were first cleaned, as prescribed by Vanderhoff Et al. (1970) and Pelton (1977), by washing four times with a strong base (3M NaOH), a strong acid (3M HCl), hot water, methanol and Millipore water in that order.

The ion exchange resins used were BioRad AG 1-X4 anion and BioRad 50W-X4 cation exchange beads, which when combined made a mixed bed ion exchange system. The resins were conditioned in bulk and stored in the dark at 5 °C for future use. The cationic resin was left in the H+ form so it would be ready for use and the anionic resin was left in the Cl- form which required treatment with a strong base and flushing with copious amounts of Millipore water before use.

NIPAM latexes were treated before titration by mixing latex with the ion exchange beads and then filtering off the ion exchange beads. The NIPAM latexes were first concentrated by ultracentrifuging the particles to a compact mass and then redis-

persing in half the original amount of Millipore water. The concentrated latexes were then mixed with ion exchange beads for one hour. The ratio of ion exchange beads to latex was roughly 1ml of each type of beads for every 5ml of concentrated latex. After stirring for one hour the ion exchange beads were carefully removed by filtering with a regular filter and filter paper .

The conductivity of the clean latex was very low so a little pottasium chloride was added to raise the conductivity to about 100 mS. The conductivity of the solution had to be high enough so that the pH meter would be stable and the curves produced by the conductivity measurements would have clearer end points.

3.5.2 Running Titrations

Simultaneous potentiometric and conductiometric titrations were performed on the latex using Aliquot a titration program developed by R.H. Pelton at McMaster University. Aliquot runs on an IBM AT and uses (Radiometer ABU Triburette) automatic burettes to dispense exact amounts of the titrants.

The latexes were titrated with 0.01 M solutions of NaOH and HCl made up from (Fisher) standard solutions. To prevent carbon dioxide from contaminating the NaOH solution the bottle which contained the NaOH was capped with a cover which contained soda lime (a mixture of sodium hydroxide and calcium oxide).

The clean latex was placed in a temperature controlled beaker which was fitted

with a cover which had several holes in it for the addition of acid and base, pH and conductivity measurements and a nitrogen line (see Figure 3.3). Nitrogen was blown into the latex for one hour to remove carbon dioxide and was then blown gently on to the surface of the latex to maintain a nitrogen atmosphere. The burettes were flushed so that no air bubbles would be in the lines and the feed lines were rinsed of excess acid or base and then placed into the latex.

The pH electrode (Fisher) was a combination of calomil electrode with a glass reference electrode. The tip of the reference electrode was covered by a jacket which was filled with a KCl solution with the same concentration as the latex to prevent leakage of salt solution into the latex which would distort the conductivity measurements. The two pH electrodes were placed in the latex.

The conductivity meter (Radiometer CDM83) was calibrated using a conductivity standard (YSI Incorporated) and then placed into the latex. A temperature probe which also attached to the conductivity meter was put into the latex to make sure the temperature remained constant.

The titration parameters were set in Aliquot and the titration was allowed to run overnight. Aliquot accepts values for the step size of acid and base addition, the maximum amount of acid and base to add per pass and the number of passes to make. The step size was set as low as possible to get more accurate end points. To improve the results from the first pass a initial dose of acid was added and then the titration was started.

3.5.3 Mass of latex titrated

The mass concentration of the latex titrated was found by taking 1 ml of the latex to be titrated and placing it on a preweighed drying plate. The latex was then dried for four hours in a vacuum oven at roughly 40°C and the tray reweighed. The latex sample was taken after treatment with the ion exchange resins but before the addition of KCl so that there would be no electrolyte in the sample to add to the weight of the dry latex.

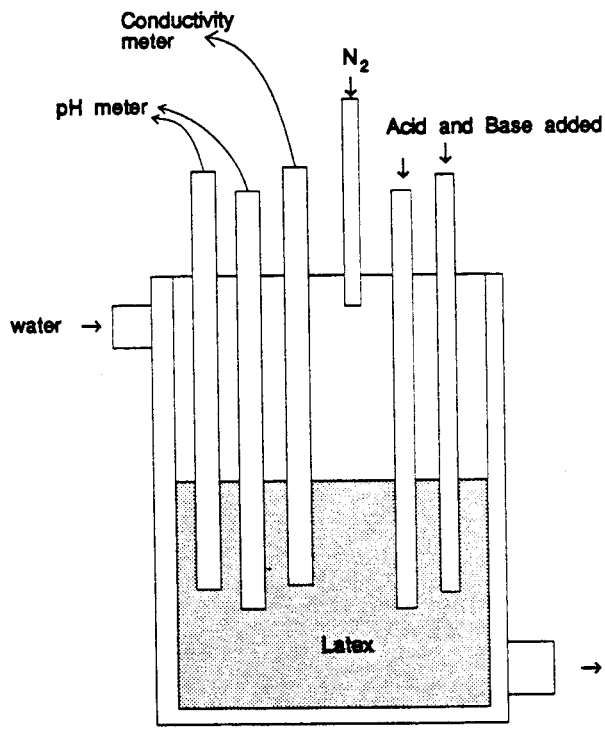

Figure 3.3 Titration Apparatus

3.6 Electrophoresis

The electrophoretic mobility of NIPAM latex particles was found by running samples on a Coulter DELSA microelectrophoresis apparatus. Dilute samples were prepared in solutions with various ion concentrations and were run at two temperatures, one below the critical temperature (at 25°C) and one above the critical temperature (at 40 °C).

Dilute samples were prepared by adding a small amount of clean latex to 10mL of the desired solution in a test tube. A vacuum was applied to the test tube to remove any dissolved air which might later form into bubbles. The electrophoresis sample cell was flushed with the solution and then filled.

The sample cell was placed in the DELSA sample chamber and the temperature of the cell was set so that the temperature at the front of the cell and at the back of the cell averaged to the desired temperature. The cell was left for 30 minutes so that the temperature gradients in the cell could stabilize.

Once the temperature was stable, measurements were made at five points across the cell. The DELSA has detectors at four angles and measurements were made at all four angles. It was necessary to make five measurements across the cell because electro-osmosis causes a parabolic flow profile to develop in the cell. The five measurements were fit to the parabolic flow equation for a closed cell (the Komataga equation) to find the electrophoretic mobility. The mobilities found at the four angles were then averaged

to get a value for the mobility of the particle in the particular solution used and at the set temperature. (A more indepth description of the analysis used is included in Appendix D.)

4 Results and Discussions

4.1 Polymerization

A number of reactions were carried out to try to develop a series of poly (NIPAM) polymerization recipes which would produce latexes which were stable, monodisperse and less than one micron in diameter. Latexes with these properties should be easy to measure using traditional colloid experimental techniques.

A table of the recipes which were made is presented in Figure 4.1. The latexes resulting from these recipes are classed as stable or unstable and polydisperse or monodisperse. The only recipes which met the requirements of stability and monodispersity were those that included surfactant (SDS). All variations that were tried without surfactant were either unstable or polydisperse or both.

The NIPAM particles which are formed in the reaction are at a reaction temperature which is above the LCST (70°C) so any SDS present will adsorb onto the surface of the particles and provide stability to the growing particles. Higher concentrations of SDS present in the reaction should provide greater levels of stabilization to the growing particles and so smaller particles. As expected, the recipes with higher concentrations of SDS produced smaller particles (as shown in Figure 4.2).

The size of the poly (NIPAM) latex particles approaches to a minimum value as the SDS concentration is increased. At some high level of SDS it is possible that the particles will be completely stabilized by the SDS as soon as they grow from soluble oligomers to insoluble globules. In this case Homogenous Nucleation kinetics could be simplified by removing the terms for the coagulation of small particles to form larger ones.

A value for the amount of SDS to include was chosen at 0.118g/l and a series of polymerizations were done where the only variable which was changed was the amount of cross-linking agent. The particle sizes of these latexes is shown in Figure 4.3.

The size of the particles at 40°C shows a general increase as the amount of cross-linker is increased. Above a weight fraction of cross-linking agent of 20wt%, the stability decreased and the particles became unstable so that some large clumps formed on the sides of the reaction vessel. At the other extreme, with no cross-linking agent included, it was found that particles still form and do not dissolve when the temperature is lowered below the transition temperature. This would indicate that there is some gel formation even when there is no cross-linker present during the polymerization. A possible explanation of this is that some branching of the poly (NIPAM) chains occurs. Thomas and Tang (1985) noted that acrylamide polymers are susceptible to crosslinking at temperatures greater than 67°C as a result of radical attack on the polymer backbone. Poly (NIPAM) may also be susceptible to crosslinking by the same mechanism at the reaction temperature of 70°C.

Experiment Number	Concentration (g/l) NIPAM	BA	(%)	KPS	SDS	Result Stable	Dispersity
05-40	14	1.4	10	0.56	0	no	poly
05-61				0.84		no	poly
05-64				1.12		no	poly
05-63				1.26		no	poly
05-62				1.68		no	poly
05-61	14	1.4	10	0.84	0	no	poly
05-65	9.33	0.933				no	poly
05-66	7	0.7				no	poly
05-40	14	1.4	10	0.56	0	no	poly
05-70					1.154	yes	mono
05-72					0.577	yes	mono
05-75					0.188	yes	mono
05-76					0.21	yes	mono
05-77					0.06	yes	mono
05-79	14	0.14	1	0.56	0.188	yes	mono
05-85		0.42	3			yes	mono
05-80		0.7	5			yes	mono
05-87		0.98	7			yes	mono
05-75		1.4	10			yes	mono
05-89		2.1	15			yes	mono
05-78		2.8	20			yes	mono
05-83		3.5	25			no	mono
05-82		4.2	30			no	mono
05-81		5.6	40			no	mono
12-83	14	0	0	0.56	0.188	Stable Particles	mono

Figure 4.1 Summary of Latex Preparation

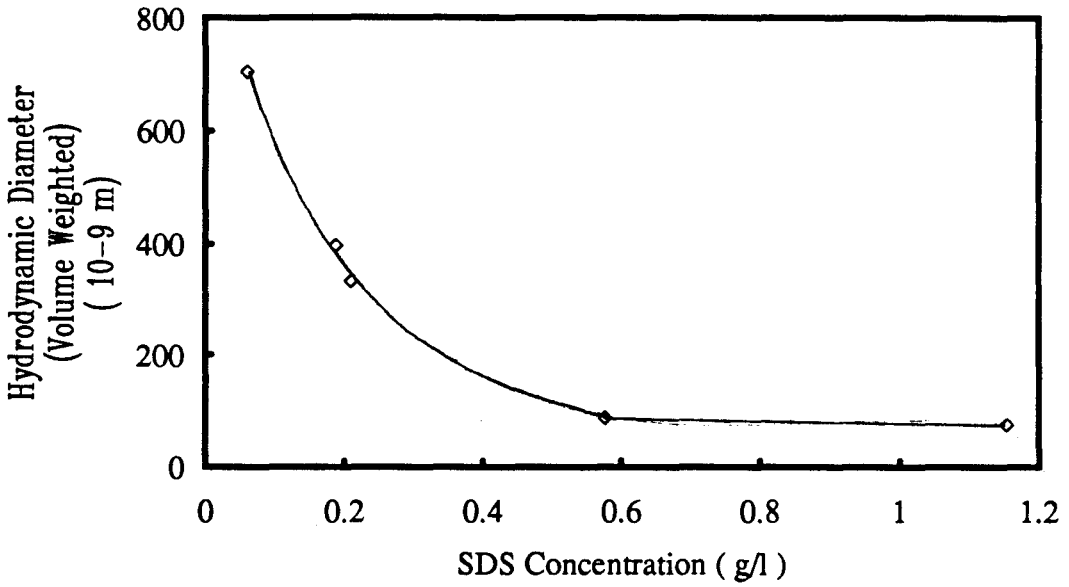

Figure 4.2 Diameter of poly (NIPAM) latex particles at 25C as a function of the SDS concentration used in the latex preparation. (the line is a rough fit to the data points)

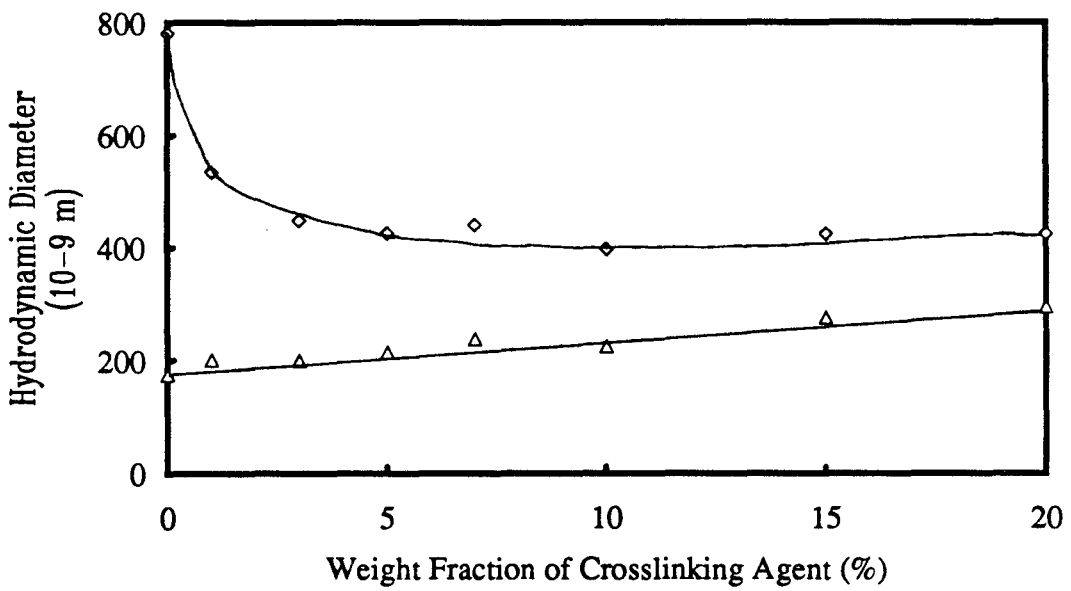

Figure 4.3 Diameter of poly (NIPAM) latex particles at 25°C (diamonds) and 40°C (triangles) produced with a range of weight fractions of crosslinking agent. (the lines are a rough fit to the data points)

4.2 Volume Fraction of Polymer in poly (NIPAM) Latex Particles

The volume fraction of polymer in a poly (NIPAM) gel latex with a weight fraction of BA of 10% was found by centrifuging the latex into a compact mass at 20°C and then determining the water content of the latex bed. The water content of the latex bed was determined by weighing a sample of the gel mass and drying the gel in a drying oven and then weighing the dry polymer.

The volume fraction of polymer can be found by applying the mass of the wet gel and the mass of the dry polymer to equation:

$$\frac{V_P}{V_T} = \frac{M_P/\rho_P}{(M_T - M_P)/\rho_W + M_P/\rho_P} \qquad \textbf{2.8}$$

which assumes that the gel is completely compacted and no interstitial volume is present or by applying the masses to equation:

$$\frac{V_P}{V_T} = \frac{1}{1-\varepsilon} \times \frac{M_P/\rho_P}{(M_{GEL} - M_P)/\rho_W + M_P/\rho_P} \qquad \textbf{2.11}$$

which assumes that the particles are compressed into a bed of regularly packed spheres which has a definable interstitial volume or porosity (ε).

The mass of wet gel and dry polymer for two experiments is shown in Figure 4.4. The volume fraction of polymer in the latexes can be calculated for both assumptions; close packed spheres and complete deformation of the gel particles.

The volume fraction of polymer found at 20°C can be extrapolated to other temperatures using the measured values for the hydrodynamic diameter of the latex particles. Estimations for the volume fraction of polymer at several temperatures are included in Figure 4.5. These results seem to indicate that assuming regularly packed spheres would give impossible results for the volume fraction of polymer at temperatures of 40°C and higher.

The calculation of volume fraction of polymer has several inherent errors which can effect the results. One, already discussed, is the packing arrangement of the gel particles. The particles could behave like solid spheres and pack in an ordered array or they could behave like mushy balls and deform to fill all of the available volume in the compact gel mass or they could behave in a way which is in between these two extremes.

When the gel latexes were centrifuged a iridescent pattern was noticed in the compact gel mass. This would indicate some sort of ordered packing arrangement but results show that the assumption of hard spheres would give values of volume faction of greater than 100 percent at temperatures of 40°C and higher. The iridescent patterns could also result if the particles were only partially deformed.

Another explanation is that the particles contain non uniform distributions of cross-linking agent within the particle. A compact gel of these particles might have regular regions of high and low cross-linking density which would have different optical densities and might give an iridescent pattern.

Another source of error which must taken in to account when doing volume fraction of polymer calculations is that the wet gel mass which is removed from the centrifuge tube may contain water which is not part of the gel but is some of the supernate liquid. A third source of error is that the dry polymer may not be completely dry and may still contain some water. Repetition of the volume fraction experiment (see Figure 4.4) shows that the results are repeatable which gives some confidence that the errors in removing a wet gel mass and drying the polymer are small.

A value for the volume fraction of polymer in the poly (NIPAM) gel latexes is required to perform calculations on gel swelling so the assumption of complete deformation will be used to calculate an approximate value for the volume fraction. The temperature at which a value for the volume fraction of polymer is most useful is at the reference point for the calculation of swelling ratios. The volume fraction of polymer at 40°C can be estimated at 77±12%.

Experimental Results			Volume Fraction of Polymer	
Exp#	Mass Wet Gel (g)	Mass Dry Polymer (g)	Assume Close Packed	Assume Complete Deformation
5-143a	0.612	0.0725	0.151	0.112
5-143b	0.9799	0.1537	0.200	0.148
Ave			0.175	0.130

Figure 4.4 The mass of wet gel and dry polymer found by experimentation and the corresponding values calculated for the volume fraction of polymer in the gel particles based on the indicated assumptions

Temperature (°C)	Diameter (10-9m)	Volume Fraction of Polymer	
		Assume Close Packed	Assume Complete Deformation
20	407	0.18	0.13
25	391	0.2	0.15
30	364	0.25	0.18
35	272	0.59	0.44
40	225	1.04	0.77
50	216	1.17	0.87

Figure 4.5 Volume fraction of Polymer in poly (NIPAM) latexes at the indicated temperatures extrapolated from the value found at 20°C.

4.3 Gel Swelling

The swelling of a polymer is usually characterized by the ratio of the total swollen volume to the volume of polymer in the gel. In cases where the volume of polymer can only be estimated, the swelling can be characterized by finding the volume of the swollen gel at the condition of interest to the volume of the gel at some reference condition For spherical gel particles the volume ratio is the cube of the diameter ratio, $V/V_R = (D/D_R)^3$, where R denotes the reference condition. Since the physical parameter measured to investigate poly (NIPAM) gels is the hydrodynamic diameter, the swelling of these gels can be characterized by a diameter swelling ratio (D/D_R).

The variable of most interest in the investigation of poly (NIPAM) gels is the temperature. The swell-shrink transition which occurs around 32°C can be characterized by the swelling which occurs across the transition. A reference temperature above the transition temperature was chosen at 40°C and the swelling ratio which was used to characterize the poly (NIPAM) gels was the ratio of the hydrodynamic diameter of the gel particles at 25°C to the diameter at the reference temperature of 40°C. That is the swelling ratio is $D_{25°C}/D_{40°C}$.

4.3.1 Effect of Ionic Strength on Gel Swelling

Swelling of a non-ionic gel is usually not dependent on the ionic strength of the surrounding solution but, since poly (NIPAM) microgels have charged groups attached, the effect of the ionic strength on the swelling of the particles must be investigated.

The diameter of the particles was measured in several solutions of KCl and HCl, at temperatures above and below the transition temperature, by dynamic light scattering. The results are presented in Figures 4.6a for results at 25°C and 4.6b for results at 40°C.

The size of the particles is shown to decrease with increasing ionic strength. At low ionic strength the charges on the particle interact and repel each other. This force of repulsion works to expand the volume of the gel particles. At higher ionic strength the interaction of the charges on each particle is reduced by the high ionic strength. At an ionic strength of 10^{-2} M KCl or HCl the interaction of the charges on the poly (NIPAM) particles is reduced to a level where the particles are no longer charge stabilized. At this ionic strength the particles are only sterically stabilized and so the particles will coagulate if the temperature is raised above the transition temperature.

The swelling ratio ($D_{25°}/D_{40°}$) however is only slightly effected by the ionic strength (as shown in Figure 4.7). In order to reduce the effects of the charged groups on the results for the swelling of the poly (NIPAM) gel latex particles, the subsequent measurements of gel swelling were performed in 10^{-3}M KCl.

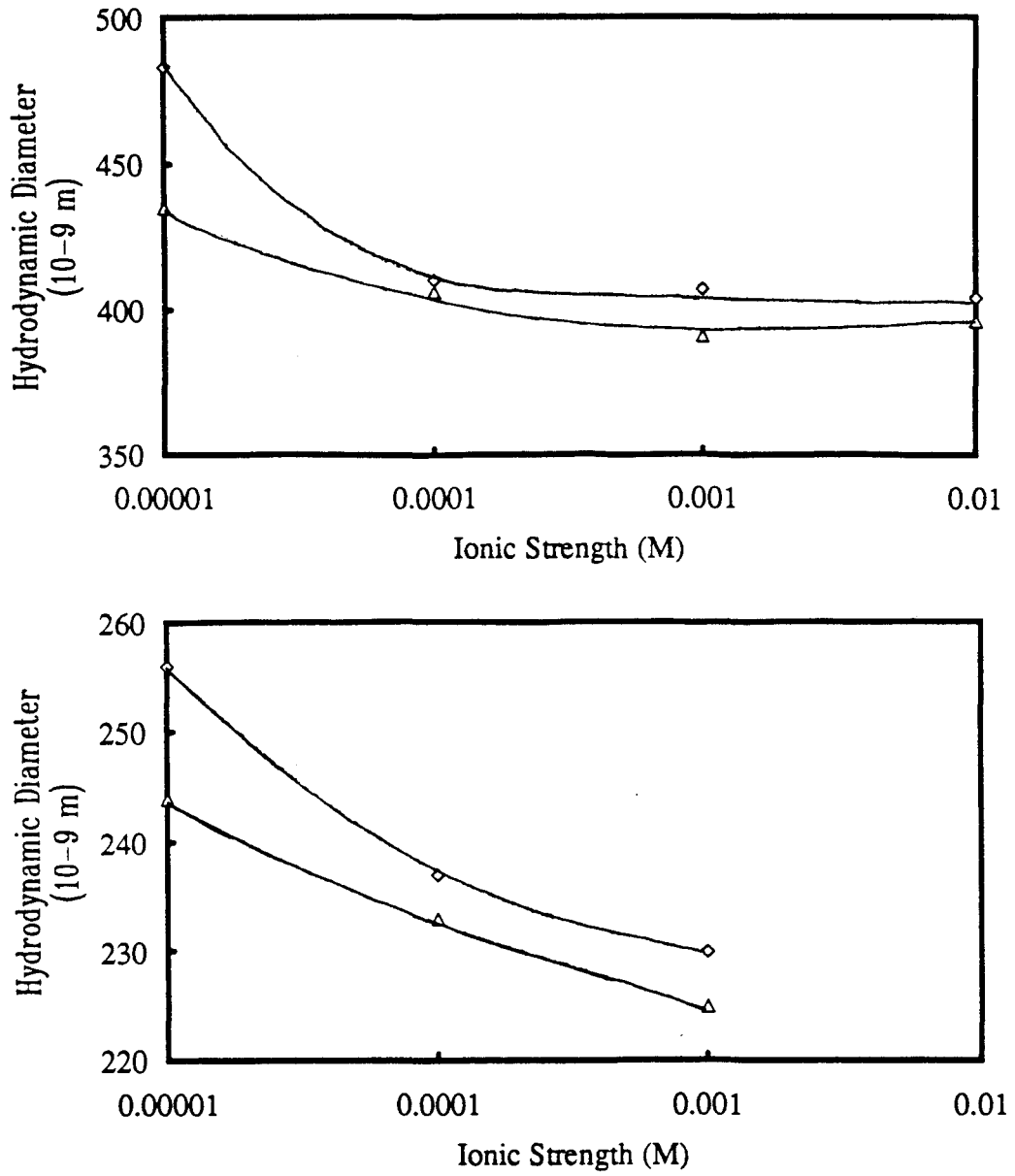

Figure 4.6 Hydrodynamic Diameter of poly (NIPAM) particles in KCl (Diamonds) and HCl (Triangles) at 25°C (a) and at 40°C (b)

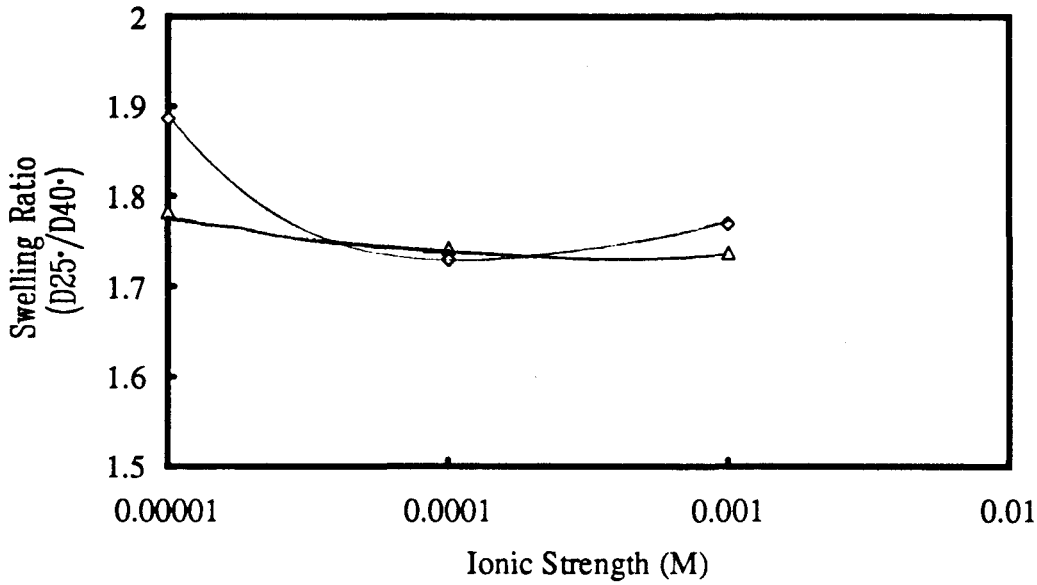

Figure 4.7 Swelling ratio of poly (NIPAM) particles in KCl (Diamonds) and HCl (Triangles)

4.3.2 Effect of Temperature on Gel Swelling

The most interesting property of poly (NIPAM) gels is the transition from a water swollen gel to a shrunken gel which occurs at about 32°C. Dynamic light scattering results on a 10% weight fraction BA poly (NIPAM) latex sample show that this transition also occurs in gel colloidal particles where the transition occurs between 30 and 40°C (see Figure 4.8).

The swelling of a cross-linked polymer gel in a solvent is dependent upon the interaction of the polymer molecules and the solvent molecules. This interaction can be expressed by the Flory-Huggins Interaction Parameter (χ). A value for χ can be found from swelling data by applying equation 2.5 which was developed in section 2.4;

$$\frac{V_1 \rho_p}{MW_{BA}} \times \frac{1}{1 + \frac{W_{NIPAM}}{W_{BA}}} \times \left(\left(\frac{V_p}{V_T} \right)^{1/3} - \frac{V_p}{2V_T} \right) = \left[\ln\left(1 - \frac{V_p}{V_T}\right) + \frac{V_p}{V_T} + \chi \left(\frac{V_p}{V_T} \right)^2 \right] \qquad (2.5)$$

To solve for χ it is necessary to approximate the volume fraction of the polymer in the gel (i.e.. V_p/V_T). The results in section 4.2 give a value for the volume fraction of polymer in the gel particles at 40°C of 77±12%.

Hirotsu (1987) further defined the Flory-Huggins Interaction Parameter by fitting χ data at different temperatures to a formula for the χ parameter which included an enthalpic and entropic contribution;

$$\chi=k(\Delta h/T-\Delta s) \qquad (2.1)$$

where k is Boltzmann's constant, Δh is the enthalpic contribution, T is the temperature in Kelvin and Δs is the entropic contribution. The results for χ can be plotted against reciprocal temperature (see Figure 4.9). The values for Δh and Δs can be found from a linear fit of χ and 1/T from equation 2.1, where $k\Delta h$ is equal to the slope and $-k\Delta s$ is equal to the y-intercept.

The results (presented in Figure 4.10) do not compare well with the results of Hirotsu (1987). Hirotsu's samples were made with about 1% BA and these results are from a sample with 10% BA. The difference in the cross-linking density could have an effect on the values found for χ, Δh and Δs.

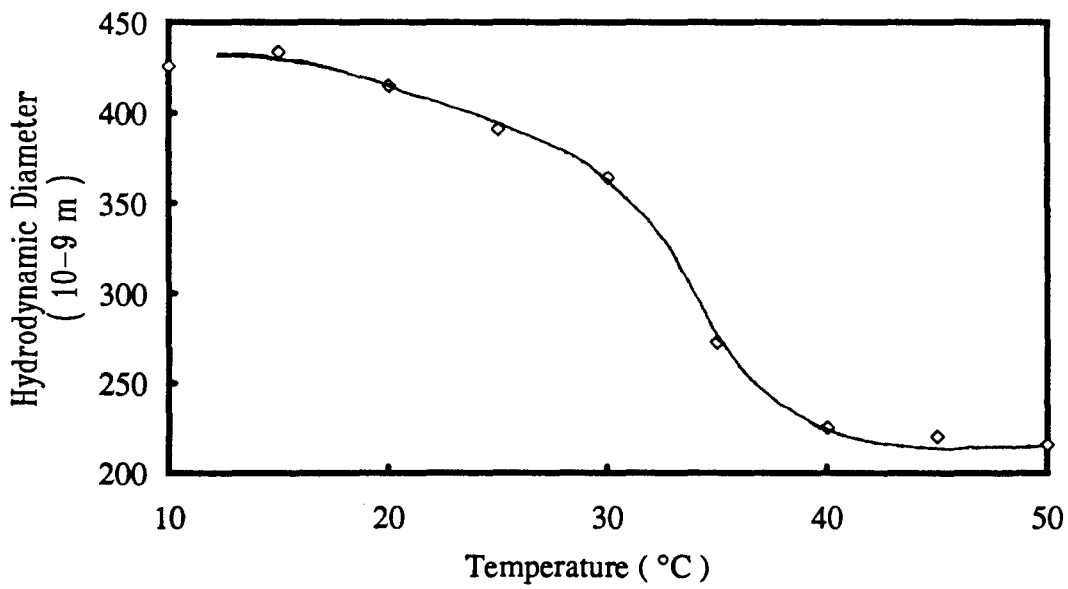

Figure 4.8 The hydrodynamic diameter of 10% BA poly(NIPAM) latex particles showing the swell/shrink transition which occurs at about 32°C

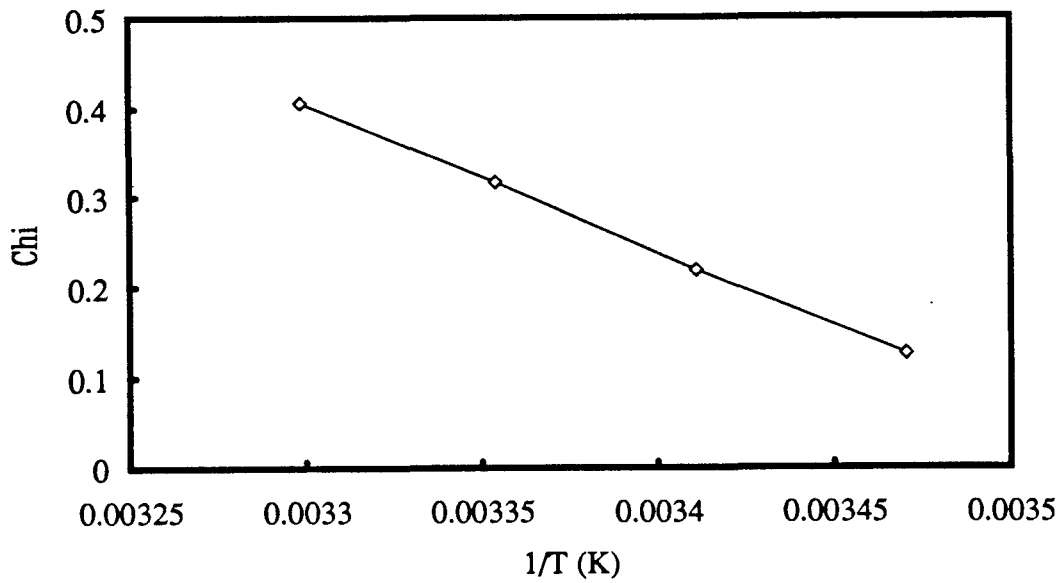

Figure 4.9 Values for the Flory-Huggins Interaction Parameter (χ) found from swelling data of a 10% BA poly (NIPAM)latex at four temperatures from 15 to 30°C

Poly (NIPAM) Gel Sample	Δh ($x10^{-20}J$)	Δs ($x10^{-23}J/K$)	χ at 25°C
Results assuming 77% volume fraction of polymer at 40°C	-2.3 ± 0.6	-8 ± 2	0.39
Hirotsu's results (1987)	-1.3 ± 0.5	-4.5 ± 1	0.19

Figure 4.10 Values for the enthalpic (Δh) and entropic (Δs) contributions to χ and estimated values for χ at 25°C for a 10% BA poly (NIPAM) latex and values from Hirotsu (1987) for a 1% BA poly (NIPAM) bulk gel

4.3.4 Effect of Cross-linking Density on Gel Swelling

The swelling ratio was found for poly (NIPAM) latex samples with cross-linking weight fractions from 1 to 20% BA. By using the value for c found for the 10% sample, the expected swelling ratio for the other cross-linking fractions was estimated using equation 2.5. The experimentally determined swelling ratios are compared with the theoretical values in Figure 4.11. The theory fits the trend of the data points but under estimates the swelling below 10% and over estimates the swelling above 10% BA. The composition of the polymer changes as the weight fraction of BA changes so it is possible that the value for χ is also changing which could account for the difference between theory and experimentation.

The values of χ were estimated for the latex samples with different cross-linking fractions and the results are presented in Figure 4.12. The results indicate that the Flory-Huggins Interaction Parameter χ increases as the amount of BA is increased. The value for χ at 1% BA found by the least squares fit of the data in Figure 4.12 is about χ=0.24 which is much closer to the value found by Hirotsu (1987) of χ=0.19 than the value for χ found for the 10% BA sample.

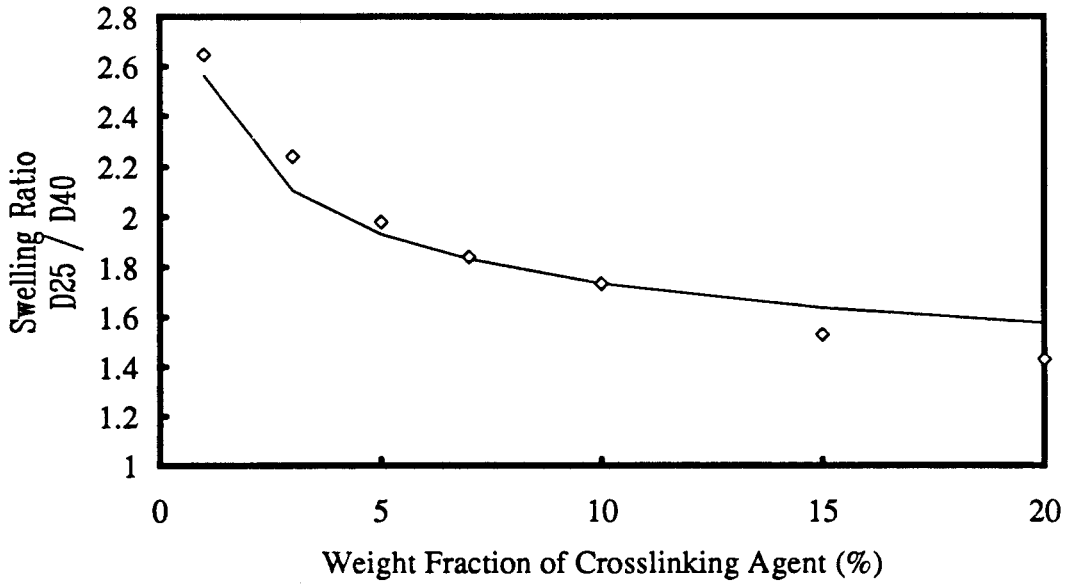

Figure 4.11 Values for the swelling ratio of poly (NIPAM) latexes compared to the estimated values for the swelling ratio found using the value for χ calculated for the 10% BA sample.

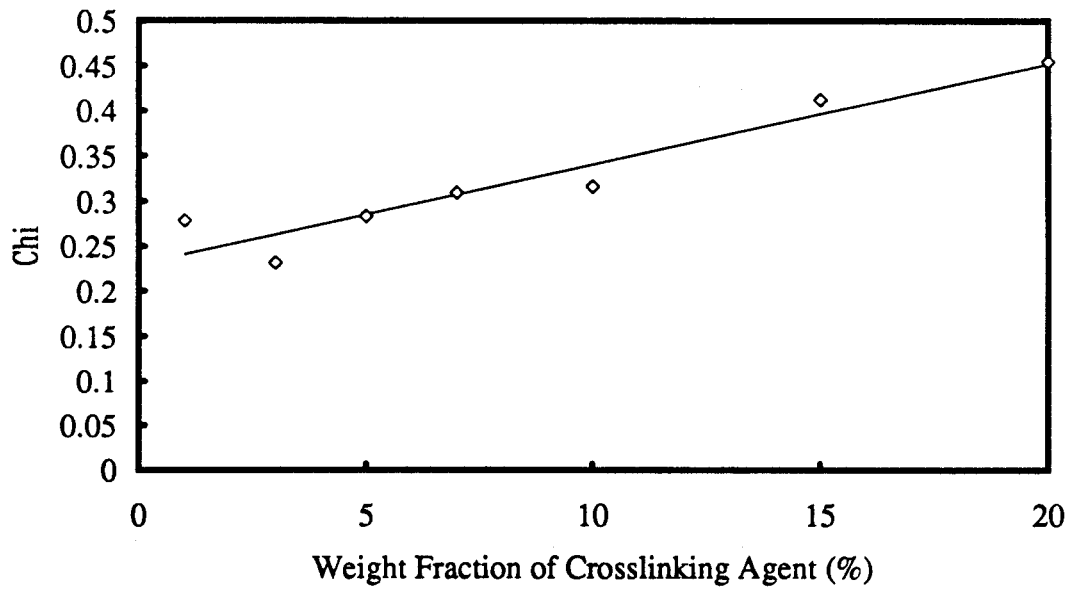

Figure 4.12 Values for χ calculated from the swelling ratio data for poly (NIPAM) latexes. The line is a least squares fit to the data points.

4.4 Titrations of Poly (NIPAM) Latexes

Simultaneous potentiometric and conductometric titrations were performed on a 10% BA poly (NIPAM) latex sample to investigate the quantity and type of charged groups attached to the particle. The types of charged groups attached to the particle are limited to sulfate (SO_4^-) end groups and carboxylic (CO_2^-) end groups. The sulfate end groups originate with the potassium persulfate initiator and the carboxylic end groups form as a result of the hydrolysis and subsequent oxidation of the polymer chain at the sulfate end group.

Several titrations were performed in order to develop an experimental procedure which would provide reproducible and accurate titration results. One successful titration, experiment number 12-67, provided initial values for the total level of charged groups on the particle and estimates for the amounts of carboxylic and sulfuric charged groups on the particle.

Another titration, experiment number 12-76, was performed with different experimental conditions in order to acquire more accurate results. The conductivity of the solution to be titrated was kept lower than previous titrations in order to increase the accuracy of the conductivity meter. The step size of the titration was also reduced in order to get more accurate values for the end points of the titration.

The results for titration 12-76 are shown in Figure 4.13. The pH and conductivity curves appear to have no clear end points but further analysis shows that quite clear end

points can be found. The slope of the pH curve was calculated from the pH data (see Figure 4.14) and shows a maximum value which corresponds to the total amount of charge in the titration.

The end points on the conductivity curve can be found by extrapolating the straight line portions of the curve on either side of the inflection. Another line can be extrapolated from the straight line section at the bottom of the inflection. The end points are found from the intersections of these lines (as shown in Figure 4.15).

The first intersection indicates the quantity of strong acid charged groups which in this case is the quantity sulfate charged groups. The second intersection indicates the total amount of charged groups present. The quantity of weak acid charged groups which in this case is the quantity of carboxylic charged groups can be found from the difference between the two intersections.

The results from both titrations, 12-67 and 12-76, are presented in Figure 4.16. The results from titration 12-76 are converted from 10^{-3}Eq to other units which may be more applicable. The volume of the samples titrated was 0.1L which can be used to convert the quantities of charged groups into units of υmol/L. El-Asser (1983) and Per Stenius (1983) both estimate the minimum error in titrations of latex particles to be about 10 to 20 υmol/L, as a result of impurities in the system. The results from these titrations give values for total charge which are well above these minimum error limits which makes it likely that the titrations are actually measuring the charges on the particles and not just impurities in the titration system.

The mass concentration of latex in titration 12-76 was measured, by drying a sample of the latex which was titrated, and found to be 25.5 g/L. This mass concentration of latex can be used to convert the quantity of titrated charged groups to Coulombs of charged groups per gram of poly (NIPAM) (see Figure 4.16).

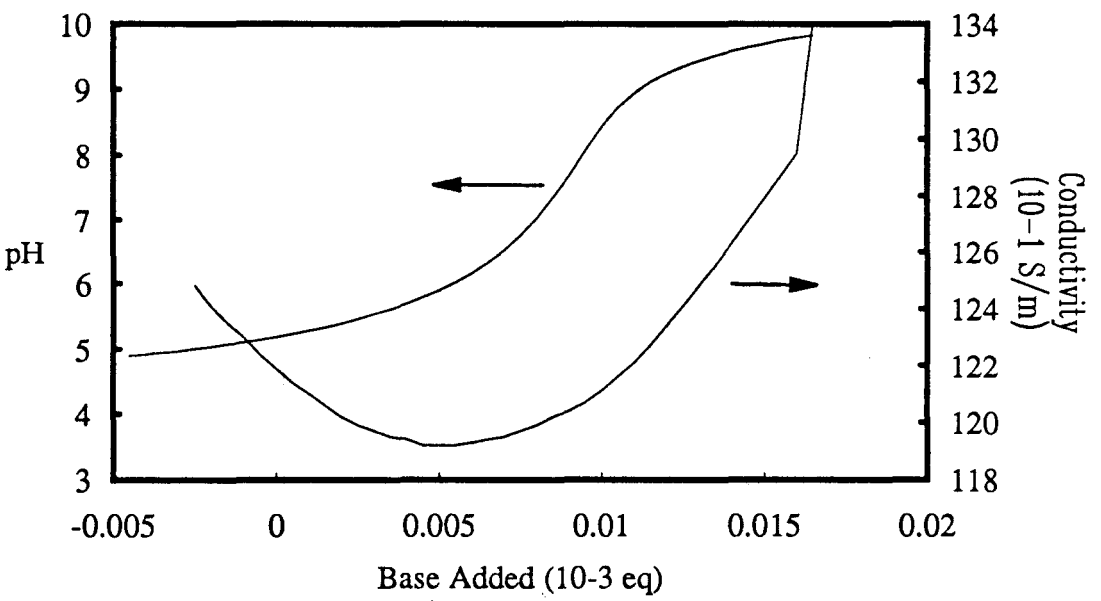

Figure 4.13 Results from a potentiometric and conductometric titration of a 10 wt% BA poly (NIPAM) latex sample.

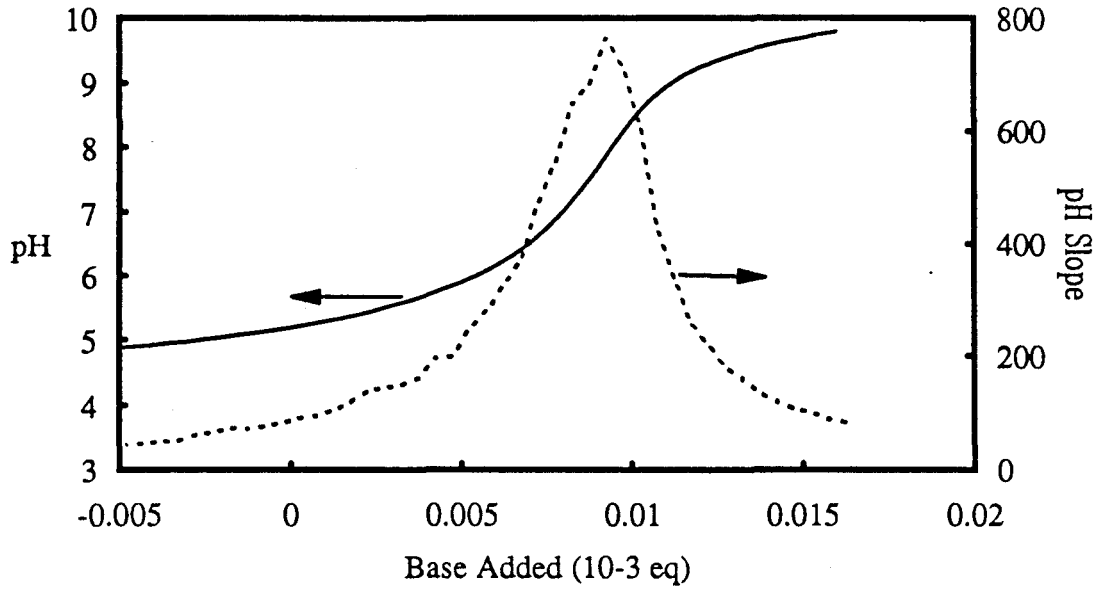

Figure 4.14 Results from the potentiometric titration showing the slope of the pH curve which indicates the end point of the titration.

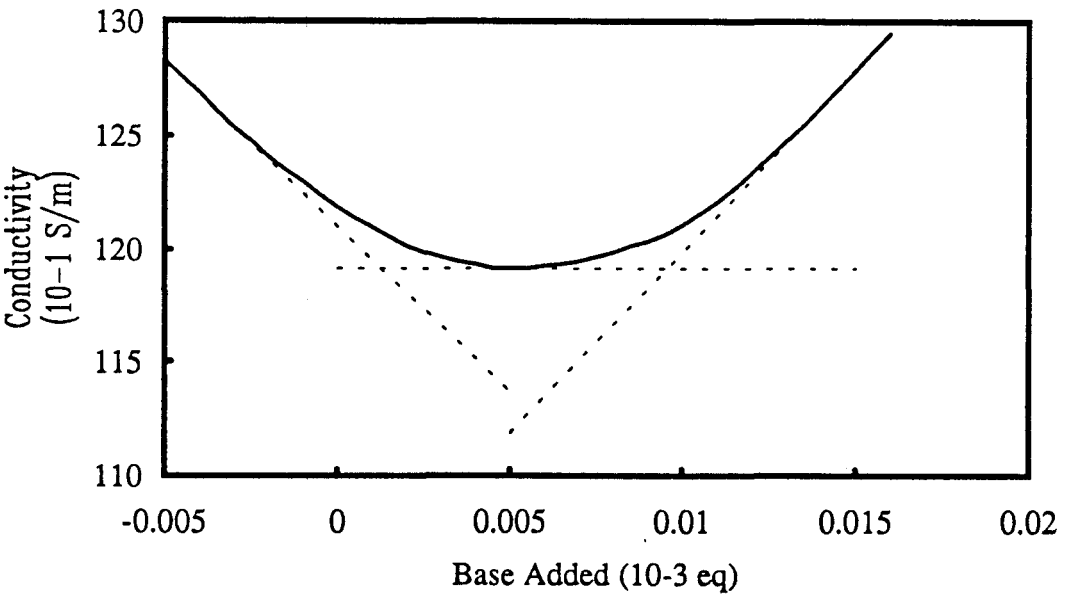

Figure 4.15 Results from the conductometric titration with extrapolations of the straight line segments of the curve. The two intersections of the lines indicate the strong and weak acid end points.

Titration	12 - 67	12 - 76			
	(10^{-6}Eq)	10^{-6}Eq	10^{-6}Mol/L	Coul/L	Coul/g
Condiometric					
SO_4^- charges	1.2	1.25	12.5	1.2	0.047
CO_2^- charges	8.3	8.31	83.1	8.0	0.31
Total charge	9.5	9.56	95.6	9.2	0.36
Potentiometric					
Total Charge	9.5	9.55	95.5	9.2	0.36

Figure 4.16 Results from two titrations presented in several units of measurement.

4.5 Electrophoresis of poly (NIPAM) Latexes

Further investigation of the nature of the charged groups on the poly (NIPAM) latex particles was done by particle electrophoresis. The electrophoretic mobility of a poly (NIPAM) latex with a weight fraction of cross-linking agent of 10% was found at temperatures above and below the transition temperature and in several KCl solutions.

Above the transition temperature, at 40°C, the electrophoretic mobility decreased as the ionic strength of the KCl solution was increased (as shown in Figure 4.17). Early electrophoresis theory indicated that the curve of mobility versus ionic strength should result in a straight line but most systems studied show a mobility versus ionic strength curve which levels off at low ionic strength (Hiemenz, 1986) as shown for the poly (NIPAM) sample above the transition temperature.

The surface charge can be estimated by using O'Brien and White's (1978) theory and their computer program which makes calculations based on their theory. The surface charge was estimated using O'Brien and White's computer program and the total charge assuming all charged groups in the particles are at the surface was calculated using the hydrodynamic diameter of the particles (see Figure 4.18). These results are compared to the total charge calculated from the titration results (section 4.4) and the estimate for the volume fraction of polymer in a poly (NIPAM) particle at 40°C (section 4.2). The percentage of charged groups on the surface can then be estimated (Figure 4.18).

Applying O'Brien and White's theory to poly (NIPAM) particles is not very practical. O'Brien and White's theory is based on solid smooth particles with no water in the interior of the particles. Poly (NIPAM) is probably a hairy sphere with a volume fraction of water in the interior which is around 23% at 40°C. The results for surface charge from O'Brien and White's theory are not accurate but the magnitude of the answers can give some information about the position of the charged groups in poly (NIPAM) particles. The estimated percentage of charge on the surface of the particle ranges from 11 to 23%. The charges in the poly (NIPAM) particles are not restricted to the surface but are probably distributed through out the particle.

Below the transition temperature, at 25°C, the electrophoretic mobility goes through a sharp increase in the mobility as the ionic strength decreases (as shown in Figure 4.18). These results do not fit into the typical relationships seen between mobility and ionic strength. A possible explanation for these results comes from the highly swollen nature of the poly (NIPAM) particles at 25°C.

At high ionic strengths the charged groups on the poly (NIPAM) particles would be masked by the high concentration of charges in the solution and so they would have little effect on the mobility and little effect on each other. The charged groups could be on the surface of the particles or they could be in the highly swollen interior of the particle.

As the ionic strength decreases the charged groups would start to effect the mobility so an increase in the mobility would occur. The charged groups would also

begin to effect other charged groups in the particle. The charged groups would repel each other and so more of the charged groups would be pushed to the outer edges and surface of the particle. As the ionic strength of the solution decreases to very low levels (i.e.. 10-5 M KCl) the charged groups would have a strong effect on the mobility and there would also be more charged groups near the surface of the particle due to intraparticle charge repulsion.

The combined effects of increased mobility as the ionic strength is decreased and increased number of charged groups near the surface as the ionic strength is decreased could result in the dramatic increase in the electrophoretic mobility as the ionic strength is decreased observed for poly (NIPAM) particles below the transition temperature.

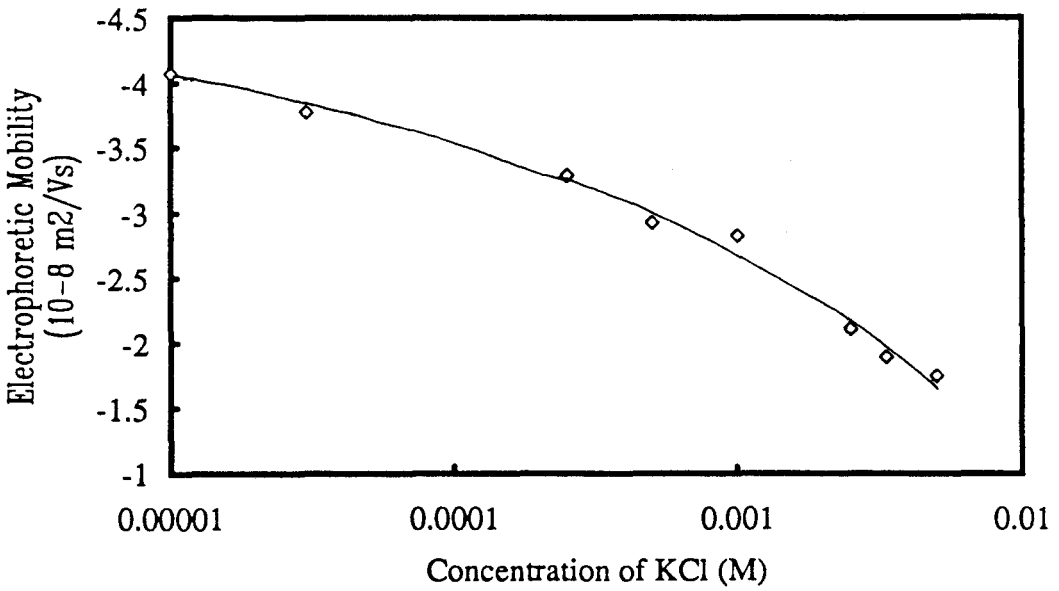

Figure 4.17 Electrophoretic Mobility of a 10 wt% BA poly (NIPAM) latex sample at 40°C in solutions of KCl.

Ionic Strength	Diameter	Electropheresis		Titration	% Charge on Surface
		Surface Charge	Total Charge	Total Charge	
	10^{-9}m	10^{-2}Coul/m^2	10^{-16} Coul/part	10^{-16} Coul/part	(%)
10^{-3}	225	0.26	4.2	18	23
10^{-4}	233	0.16	2.7	18	15
10^{-5}	244	0.10	1.9	18	11

Figure 4.18 Number of charged groups in a particle estimated from electropheresis and titration data

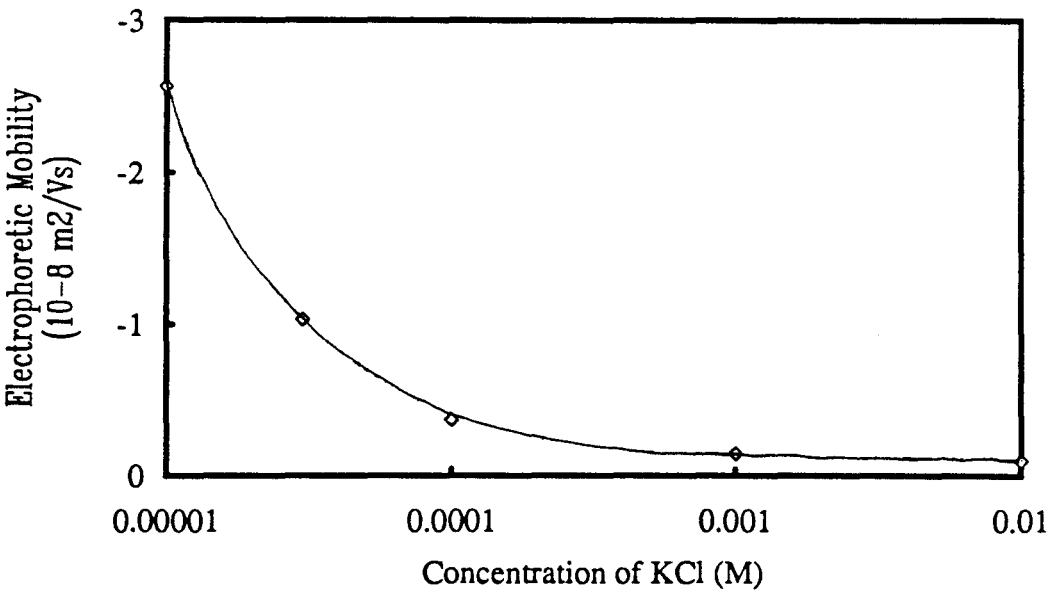

Figure 4.19 Electrophoretic Mobility of a 10 wt% BA poly (NIPAM) latex sample at 25°C in solutions of KCl.

5 Conclusions

- Monodisperse and stable poly (NIPAM) microgel particles can be prepared with weight fractions of cross-linking agent from 1 to 20% provided sufficient surfactant is present to stabilize the particles during the polymerization.

- Higher surfactant concentrations present in the poly (NIPAM) polymerization recipe result in smaller poly (NIPAM) particles.

- The poly (NIPAM) microgel latexes are swollen with water and go through a swell/ shrink transition as the temperature is raised to above about 30°C.

- The swelling of the poly (NIPAM) gels can be expressed using the Flory-Huggins Interaction Parameter χ. The χ parameter and the extent of the particle swelling are both a function of the amount of cross-linking agent in the poly (NIPAM) particles.

- Carboxylic and Sulfuric end groups are attached to the poly (NIPAM) chains at a total level of about 0.39 Coulombs per gram of polymer.

- The charged groups appear to be distributed throughout the particle.

6 Bibliography

Amiya, T., Hirokawa, Y., Hirose, Y., Li, Y., Tanaka, T., J.Chem.Phys., 86, 2375-2379, (1987)

Barth H.G. (Ed), Modern Methods of Particle Size Analysis, John Wiley & Sons, (1984)

Chiantore, O., Guaita, M., Trossarelli, L., Makromol.Chem., 180, 969-973, (1979)

Chiantore, O., Costa, L., Guaita, M., Makromol., Rapid Commun. 3, 303-309, 1982

Chiantore, O., Trossarelli, L., Guaita, M., Makromol.Chem., 183, 2257-2263, (1982)

Chow, R.S., Takamura, K., J. Colloid Inter. Sci., 125, 226-236, (1988)

Coultor Delsa Manual, Coulter Scientific Instruments, (1989)

Donath, E., Patoshenko, V., J. Electroanal. Chem., 104 534-554, (1979)

Eagland,D., Allen,A.P., J.Colloid Inter Sci., 58, No2, 230, (1977)

El-Aasser, M.S., in Poehlin, Et al.(Ed), Science and Technology of Polymer Colloids Vol 2, NATO ASI Series, (1983)

Fayed, M.E., and Otten, L., Handbook of Powder Science and Technology, Van Nostrand Reinhold Company, New York, (1984)

Feeney J.P., Napper, D.H., Gilbert, R.G., Macromolecules, 20, 2922-2930 (1987)

Flory P.J., Principles of Polymer Chemistry, Cornell University Press, (1953)

Fujishige, S., Polymer J., 19, 297-300, (1987)

Fujishige, S., Kubota, K. and Ando, I., J.Phys.Chem, 93, 3311-3313, (1989)

Goff J.R., Luner P., J.Colloid Inter Sci., 99, No2, 468, (1984)

Goodwin, J.W., Ottewill, R.H., Pelton, R.H., Yates, D.E., Brit. Polymer J., 10, 173 (1978)

Goodwin, J.W., Ottewill, R.H., Pelton R.H., Colloid & Polymer Sci. 257, 61-69 (1979)

Heskins, M., Guillet, J.E., J.Macromol.Sci., A2(8), 1441-1455, (1968)

Hiemenz, P.C., Principles of Colloid and Surface Chemistry, Marcel Dekkler Inc.,N.Y., (2nd Ed, 1986)

Hirokawa, Y., Tanaka, T., J.Chem.Phys, 81, 6379-6380, 1984

Hirokawa Y., Sato, E., Hirotsu, S., Tanaka, T., Polym.Mater.Sci.Eng., 52, 520-521, (1985)

Hirotsu, S., J.Phys.Soc.Japan, 56, 233-242, (1987)

Hirotsu, S., J.Chem.Phys, 88, 427-431, (1988)

Hirotsu, S., Hirokawa, Y., Tanaka, T., J.Chem.Phys., 87, 1392-1395, (1987)

Hirotsu, S., Japanese J.App.Phys, 24, 396-398, (1985)

Hirotsu S., J. Phys. Soc. Japan, 56, 233-242, (1987)

Hunter, R.J., Zeta Potential in Colloid Science, Academic Press, London, (1981)

Kubota, K., Fujishige, S., Ando, I., Polymer J., 22, 15-20, (1990)

Linoya, K., Beddow, J.K., Jimbo, G., Powder Technology, Hemisphere Publishing Corporation, Washington D.C., (1984)

MacWilliams, D.C., in Yocum, R.H. and Nyquist, E.B., Functional Monomers, Marcel Dekker Inc., New York, (1973)

Midmore, B.R., Hunter, R.J., J.Colloid Inter Sci., 122, No2, 521, (1988)

David Nicoli, Private Phone Conversation (April, 1990)

NICOMP 370 Submicron Particle Sizer Manual, Pacific Scientific, (1978)

O'Brien R.W., White L.R., J. Chem. Soc. Faraday Trans 2, 74, 1607, (1978)

Ohshima, H., Healy, T.W., White, L.R., J. Chem. Soc., Faraday Trans. 2, 80, 1643, (1984)

Ohshima, H., Kondo, T., J. Colloid Inter. Sci.,116 No2, 305-311, (1987)

Pelton, R.H., Chibante, P., Colloids and Surfaces, 20, 247-256, (1986)

Pelton, R.H., Pelton, H.M., Morphesis, A., Rowell, R.L., Langmuir, 5, 816-818, (1989)

Stenius, P., Kronberg B., in Poehlin, Et al.(Ed), Science and Technology of Polymer Colloids Vol 2, NATO ASI Series, (1983)

Tanaka, T., Sato, E., Hirokawa Y., Hirotsu, S., Peetermans, J., Phys.Rev.Let., 55, 2455-2458, (1985)

Thomas, W.M., Wang, D.W., in Kroschwitz, J.I.(Ed.), Encyclopedia of Polymer Science and Engineering, John Wiley & Sons, New York, (1985)

Vanderhoff Et al., in Goldfinger, G. (Ed), Clean Surfaces: Their Preparation and Characterization for Interfacial Studies, Marcel Dekker Inc, New York, (1970)

Vold, R.D. and Vold M.J., Colloid and Interface Chemistry, Addison-Wesley Publishing Company, Inc., (1983)

Volk H., Friedrich, R.E., in Davidson, R.L. (Ed), Handbook of Water-Soluble Gums and Resins, McGraw-Hill Book Company, New York, (1980)

Ware, B.R., and Flygare, W.H., J. Colloid Interface Sci., 39, 670 (1972)

Wiersema, P.H., Loeb, A.L., Overbeek, J.Th.G., J.Colloid Interface Sci., 22, 78, (1966)

Zana R., J.Polymer Sci., 18, 121-126, (1980)

Zukoski C.F., Saville, D.A., J. Colloid Inter. Sci., 114, 32-53, (1986)

Zukoski C.F., Saville, D.A., J. Colloid Inter. Sci., 107, No2, 322-333, (1985)

7 Appendix

Appendix 1

Clean Latexes

In the experimental section of this thesis a technique for the cleaning of NIPAM latexes was described. The particles were ultracentrifuged into a compact gel, the supernate was poured off, and the particles were redispersed in doubly distilled water. To ensure that this technique does remove the impurities, especially the surfactant (SDS), the supernate was analysed by measuring the conductivity. The results are shown in Figure A1.1. The conductivity decreases exponentially until the fourth repeat, when the conductivity is low and the latex is considered "clean".

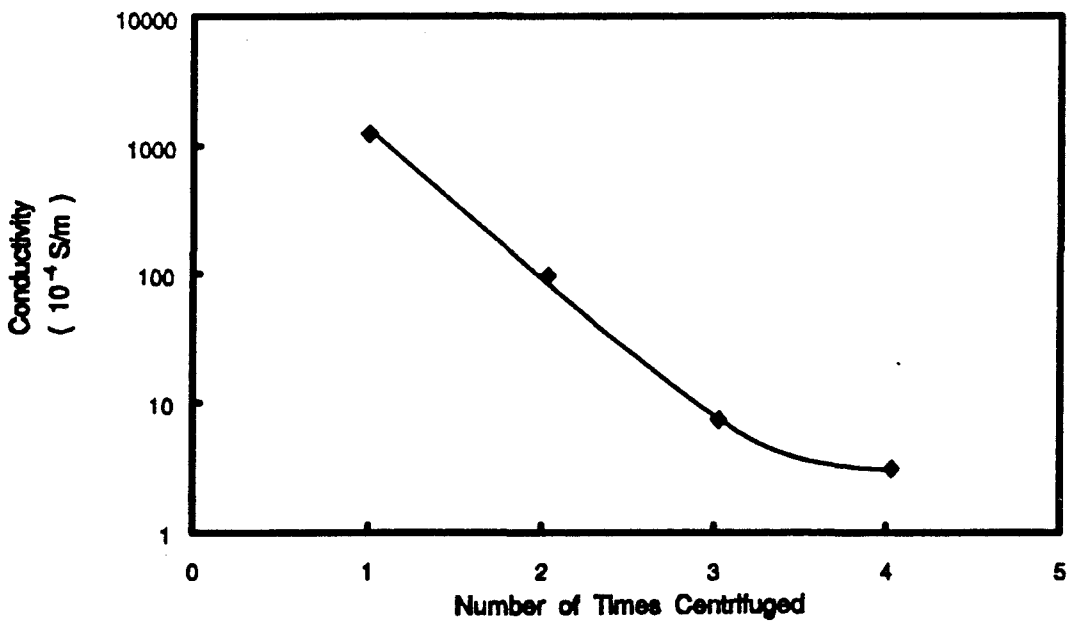

Figure A1.1 Conductivity of the supernate from the ultracentrifugation of a poly (NIPAM) latex

Appendix 2

Raw Data

SDS concentration (g/l)		D (25°C) (10-9 m)
1.154		76.2
0.577		87.9
0.188		398
0.21		334
0.06		705

Data for Figure 4.2

wt fraction BA (%)	D (25°C) (10-9 m)	Std Dev (%)	D (40°C) (10-9 m)	Std Dev (%)
0	781	60	176	40
1	535	39	202	22
3	448	14	200	4
5	426	17	215	20
7	440	28	239	32
10	398	24	225	16
15	425	30	278	25
20	425	27	297	30

Data for Figure 4.3

Ionic Strength (M)	Diameter (10-9 m) 25°C	40 °C	Swelling Ratio
[KCl]			
0.01	396		
0.001	391	225	1.74
0.0001	406	233	1.74
0.00001	435	244	1.78
[HCl]			
0.01	404		
0.001	407	230	1.77
0.0001	410	237	1.73
0.00001	483	256	1.89

Data for Figures 4.6 and 4.7

Temperature (°C)	Hydrodynamic Diameter (10-9m)
10	426.1
15	433.8
20	415
25	391
30	364.3
35	272.7
40	225.4
45	220.7
50	216.1

Data for Figure 4.8

Temperature (°C)	1/T (1/K)	Hydrodynamic Diameter (10-9 m)	Hydrodynamic Volume (10-18 m3)	VP/VT	Chi
15	0.00347	433.8	0.341945783	0.107805	0.126246
20	0.003411	415	0.299386973	0.123129	0.218334
25	0.003354	391	0.250391096	0.147223	0.316853
30	0.003299	364.3	0.202519163	0.182024	0.407137
40		225.4	0.04796786		

Data for Figure 4.9

Temperature (°C)	1/T (1/K)	Hydrodynamic Diameter (10-9 m)	Hydrodynamic Volume (10-18 m3)	VP/VT '(70%)	Chi	VP/VT '(90%)	Chi	VP/VT '(60%)	Chi
15	0.00347	433.8	0.341945783	0.107805	0.126246	0.126251	0.23371	0.091181	-0.02052
20	0.003411	415	0.299386973	0.123129	0.218334	0.144198	0.306637	0.104143	0.099057
25	0.003354	391	0.250391096	0.147223	0.316853	0.172415	0.3862	0.124522	0.22531
30	0.003299	364.3	0.202519163	0.182024	0.407137	0.21317	0.461981	0.153956	0.33792
40		225.4	0.04796786						
-1644.24419	5.830399					-1335.1	4.864391	-2099.42	7.263759
dh	-2.3E-20	Joules					-1.8E-20		-2.9E-20
ds	-8E-23	Joules/Kelvin					-6.7E-23		-1.00E-22
Boltzmanns	1.38E-23								

Data for Figure 4.10

	A	B	C	D	E	F	G	H	I
1									
2									
3	%BA	D25	D40	D ratio	Vol Ratio	Vol Ratio Calculated	VP/VT	Chi	Dratio Calculated
4									
5	0	781	176	4.4375	87.38062	87.380615	0.008795	#DIV/0!	
6	1	535	202	2.648515	18.57835	16.85	0.045608	0.3166306	2.5636966
7	3	448	200	2.24	11.23942	9.35	0.082193	0.3169246	2.1067057
8	5	426	215	1.981395	7.778815	7.23	0.106293	0.3168402	1.933657
9	7	440	239	1.841004	6.239709	6.15	0.124959	0.3167704	1.8321388
10	10	391	225.4	1.734694	5.219976	5.2199764	0.147223	0.3168527	1.7346939
11	15	425	278	1.528777	3.572995	4.385	0.175257	0.3166834	1.6367783
12	20	425	297	1.430976	2.930201	3.91	0.196547	0.3162994	1.5754051

Data for Figure 4.11

	A	B	C	D	E	F	G
15	%BA	D25	D40	D ratio	Vol Ratio	VP/VT	Chi
16							
17	0	781	176	4.4375	87.38062	0.0087949	#DIV/0!
18	1	535	202	2.648515	18.57835	0.0413653	0.278922
19	3	448	200	2.24	11.23942	0.0683754	0.2320602
20	5	426	215	1.981395	7.778815	0.098794	0.2836469
21	7	440	239	1.841004	6.239709	0.1231628	0.3101189
22	10	391	225.4	1.734694	5.219976	0.1472229	0.3168527
23	15	425	278	1.528777	3.572995	0.2150857	0.4123376
24	20	425	297	1.430976	2.930201	0.2622687	0.4550117

Data for Figure 4.12

Excess base (mEq)	pH	Conductivity	Temp.	Time	Mid point	pH slope
0.0165	9.840423	134	25	20:57	0.01675	76.281411
0.016	9.798309	129.5	25	20:52	0.01625	84.227391
0.0155	9.752752	128.7	25	20:47	0.01575	91.113908
0.015	9.701898	127.9	25	20:42	0.01525	101.70855
0.0145	9.647866	127.1	25	20:37	0.01475	108.06533
0.014	9.587211	126.3	25	20:32	0.01425	121.30863
0.0135	9.519141	125.5	25	20:27	0.01375	136.14113
0.013	9.439416	124.8	25	20:22	0.01325	159.44934
0.0125	9.348832	124.1	25	20:17	0.01275	181.16835
0.012	9.239442	123.4	25	20:12	0.01225	218.77932
0.0115	9.112306	122.7	25	20:07	0.01175	254.27137
0.011	8.942792	122.1	25	20:02	0.01125	339.02849
0.0105	8.730635	121.6	25	19:57	0.01075	424.31535
0.01	8.428952	121.1	25	19:52	0.01025	603.36477
0.0095	8.072178	120.7	25	19:47	0.00975	713.54903
0.009	7.690506	120.4	25	19:42	0.00925	763.34384
0.0085	7.348564	120.2	25	19:37	0.00875	683.88404
0.008	7.024103	119.9	25	19:32	0.00825	648.92173
0.0075	6.751291	119.7	25	19:26	0.00775	545.62398
0.007	6.513971	119.5	25	19:22	0.00725	474.63989
0.0065	6.328035	119.4	25	19:16	0.00675	371.87188
0.006	6.164083	119.3	25	19:11	0.00625	327.90412
0.0055	6.024234	119.2	25	19:06	0.00575	279.69851
0.005	5.899482	119.2	25	19:01	0.00525	249.50378
0.0045	5.799362	119.2	25	18:56	0.00475	200.2387
0.004	5.700832	119.4	25	18:51	0.00425	197.06031
0.0035	5.619518	119.5	25	18:46	0.00375	162.62773
0.003	5.545091	119.7	25	18:41	0.00325	148.8547
0.0025	5.472253	119.9	25	18:36	0.00275	145.67631
0.002	5.401798	120.2	24.9	18:31	0.00225	140.90872
0.0015	5.341939	120.6	24.9	18:26	0.00175	119.71944
0.001	5.288966	121	24.9	18:21	0.00125	105.9464
0.0005	5.24076	121.4	24.9	18:16	0.00075	96.411228
0	5.194673	121.9	24.9	18:11	0.00025	92.173372
-0.0005	5.153354	122.4	24.9	18:06	-0.00025	82.638195
-0.001	5.114419	123	25	18:01	-0.00075	77.870607
-0.0015	5.077867	123.5	24.9	17:56	-0.00125	73.103019
-0.002	5.041051	124.1	24.9	17:51	-0.00175	73.632751
-0.0025	5.007678	124.8	24.9	17:46	-0.00225	66.746235
-0.003	4.976424	125.4	24.9	17:41	-0.00275	62.508378
-0.0035	4.950732	126.1	24.9	17:36	-0.00325	51.384006
-0.004	4.926099	126.9	24.9	17:31	-0.00375	49.265078

Data for Figures 4.13, 4.14, and 4.15

Exp #	Conc KCl (M)	Conductivity (10-1 S/m)	Mobility (10-8 m2/Vs)
5-101	0.005	0.92	-1.75
5-105	0.00333	0.651	-1.89
5-103	0.0025	0.524	-2.11
12-015	0.001	0.193	-2.83
5-107	0.0005	0.1064	-2.93
5-109	0.00025	0.0548	-3.29
12-036	0.00003	0.00577	-3.78
12-034	0.00001	0.00529	-4.075

Data for Figure 4.17

Exp #	Conc KCl (M)	Mobility (10-8 m2/Vs)
12-025	0.01	-0.098
12-022	0.001	-0.1445
5130	0.0001	-0.369
12-038	0.00003	-1.031
12-026	0.00001	-2.56

Data for Figure 4.19

Appendix 3

Sample Calculations

Exp#	Experimental Results Mass Wet Gel (g)	Mass Dry Polymer (g)
5-143a	=2.2645-1.6525	=1.725-1.6525
5-143b	=2.6813-1.7014	=1.8551-1.7014
Ave		

Density poly(NIPAM)	1.07
Density of Water(20C)	1

Volume Fraction of Polymer Assume Close Packed	Assume Complete Deformation
=1/(1-0.2595)*C6/denP/((B6-C6)/denW+C6/denP)	=C6/denP/((B6-C6)/denW+C6/denP)
=1/(1-0.2595)*C7/denP/((B7-C7)/denW+C7/denP)	=C7/denP/((B7-C7)/denW+C7/denP)
=SUM(D6+D7)/2	=SUM(E6+E7)/2

denP
denW

Calculation for Figure 4.4

	A	B	C	D	E
1					
2					
3	Temperature	1/T	Hydrodynamic	Hydrodynamic	VP/VT
4	(°C)	(1/K)	Diameter	Volume	'(70%)
5			(10-9 m)	(10-18 m3)	
6	15	=1/(273.16+A6)	433.8	=4/3*PI()*(C6/1000)^3	=(Dforty*0.7685)/D6
7	20	=1/(273.16+A7)	415	=4/3*PI()*(C7/1000)^3	=(Dforty*0.7685)/D7
8	25	=1/(273.16+A8)	391	=4/3*PI()*(C8/1000)^3	=(Dforty*0.7685)/D8
9	30	=1/(273.16+A9)	364.3	=4/3*PI()*(C9/1000)^3	=(Dforty*0.7685)/D9
10					
11	40		225.4	=4/3*PI()*(C11/1000)^3	
12					
13	=LINEST(F6:F9,B6:B9)	=LINEST(F6:F9,B6:B9)			
14					
15	dh	=A13*B18	Joules		
16	ds	=-B13*B18	Joules/Kelvin		
17					
18	Boltzmanns	1.3805E-23			

Calculation for Figure 4.10

1 of 2

	F
1	
2	
3	Chi
4	
5	
6	=-((0.000018*1070000/154)*(1/(1+100/10))*(E6^(1/3)-E6/2)+LN(1-E6)+E6)/(E6^
7	=-((0.000018*1070000/154)*(1/(1+100/10))*(E7^(1/3)-E7/2)+LN(1-E7)+E7)/(E7^
8	=-((0.000018*1070000/154)*(1/(1+100/10))*(E8^(1/3)-E8/2)+LN(1-E8)+E8)/(E8^
9	=-((0.000018*1070000/154)*(1/(1+100/10))*(E9^(1/3)-E9/2)+LN(1-E9)+E9)/(E9^
10	
11	
12	
13	
14	
15	
16	
17	
18	

Calculation for Figure 4.10 cont'd.

2 of 2

	A	B	C	D	E	F	G
1							
2							
3	%BA	D25	D40	D ratio	Vol Ratio	Vol Ratio	VP/VT
4		(10-9 m)	(10-9 m)			Calculated	
5	0	781	176	=B5/C5	=D5^3	87.38061523437	=1/F5*0.7685
6	1	535	202	=B6/C6	=D6^3	16.85	=1/F6*0.7685
7	3	448	200	=B7/C7	=D7^3	9.35	=1/F7*0.7685
8	5	426	215	=B8/C8	=D8^3	7.23	=1/F8*0.7685
9	7	440	239	=B9/C9	=D9^3	6.15	=1/F9*0.7685
10	10	391	225.4	=B10/C10	=D10^3	5.219976370389	=1/F10*0.7685
11	15	425	278	=B11/C11	=D11^3	4.385	=1/F11*0.7685
12	20	425	297	=B12/C12	=D12^3	3.91	=1/F12*0.7685
13							

Calculation for Figure 4.11

1 of 2

	H	I	J	K
1				
2				
3	Chi	Dratio Calculated		
4				
5	=-((0.000018*1070000/154)*(1/(1+100/A5))*(G5^(1/3)-G5/2)+LN(1-G5)+G5)/(G5^2)			
6	=-((0.000018*1070000/154)*(1/(1+100/A6))*(G6^(1/3)-G6/2)+LN(1-G6)+G6)/(G6^2)	=F6^(1/3)		
7	=-((0.000018*1070000/154)*(1/(1+100/A7))*(G7^(1/3)-G7/2)+LN(1-G7)+G7)/(G7^2)	=F7^(1/3)		
8	=-((0.000018*1070000/154)*(1/(1+100/A8))*(G8^(1/3)-G8/2)+LN(1-G8)+G8)/(G8^2)	=F8^(1/3)		
9	=-((0.000018*1070000/154)*(1/(1+100/A9))*(G9^(1/3)-G9/2)+LN(1-G9)+G9)/(G9^2)	=F9^(1/3)		
10	=-((0.000018*1070000/154)*(1/(1+100/A10))*(G10^(1/3)-G10/2)+LN(1-G10)+G10)/(G10^2	=F10^(1/3)		
11	=-((0.000018*1070000/154)*(1/(1+100/A11))*(G11^(1/3)-G11/2)+LN(1-G11)+G11)/(G11^2	=F11^(1/3)		
12	=-((0.000018*1070000/154)*(1/(1+100/A12))*(G12^(1/3)-G12/2)+LN(1-G12)+G12)/(G12^2	=F12^(1/3)		
13				

Calculation for Figure 4.11 cont'd.

2 of 2

	A	B	C	D	E	F
15	%BA	D25	D40	D ratio	Vol Ratio	VP/VT
16						
17	0	781	176	=B17/C17	=D17^3	=1/E17*0.7685
18	1	535	202	=B18/C18	=D18^3	=1/E18*0.7685
19	3	448	200	=B19/C19	=D19^3	=1/E19*0.7685
20	5	426	215	=B20/C20	=D20^3	=1/E20*0.7685
21	7	440	239	=B21/C21	=D21^3	=1/E21*0.7685
22	10	391	225.4	=B22/C22	=D22^3	=1/E22*0.7685
23	15	425	278	=B23/C23	=D23^3	=1/E23*0.7685
24	20	425	297	=B24/C24	=D24^3	=1/E24*0.7685

Calculation for Figure 4.12

	G
15	Chi
16	
17	=-((0.000018*1070000/154)*(1/(1+100/A17))*(F17^(1/3)-F17/2)+LN(1-F17)+F17)/(F17^2
18	=-((0.000018*1070000/154)*(1/(1+100/A18))*(F18^(1/3)-F18/2)+LN(1-F18)+F18)/(F18^2
19	=-((0.000018*1070000/154)*(1/(1+100/A19))*(F19^(1/3)-F19/2)+LN(1-F19)+F19)/(F19^2
20	=-((0.000018*1070000/154)*(1/(1+100/A20))*(F20^(1/3)-F20/2)+LN(1-F20)+F20)/(F20^2
21	=-((0.000018*1070000/154)*(1/(1+100/A21))*(F21^(1/3)-F21/2)+LN(1-F21)+F21)/(F21^2
22	=-((0.000018*1070000/154)*(1/(1+100/A22))*(F22^(1/3)-F22/2)+LN(1-F22)+F22)/(F22^2
23	=-((0.000018*1070000/154)*(1/(1+100/A23))*(F23^(1/3)-F23/2)+LN(1-F23)+F23)/(F23^2
24	=-((0.000018*1070000/154)*(1/(1+100/A24))*(F24^(1/3)-F24/2)+LN(1-F24)+F24)/(F24^2

Calculation for Figure 4.12 cont'd.

Appendix 4

Experimental Procedure and Data Analysis for Coulter DELSA 440 Electrophoresis

This appendix describes some of the experimental procedures and data analysis used to acquire the electrophoretic mobility data presented in this thesis. The work here should be considered as a supplement to the Coulter DELSA 440 manual and only when it is necessary will any information from the manual be included in this appendix. A very brief introduction, describing the function of the DELSA 440, will be provided for those who are only reading this thesis and not the DELSA manual.

A4.1 Introduction to the DELSA 440

DELSA is an acronym for Doppler Electrophoretic Light Scattering Analyzer. In this introductory section, the Coulter Machine will be described, the principle of Laser Doppler Velocimetry will be introduced and the topics of Particle Electrophoresis and Electro-osmosis will be discussed.

A4.1.1 Coulter Apparatus

The Coulter apparatus is made up of several main components. These are a sample cell, a laser beam and detectors, a microscope to view the sample and a computer which does the analysis.

The sample cell (see figure A4.1) has two silver electrodes and in between the electrodes is a fused quartz block with a channel in it where the sample is placed and where the actual electrophoresis occurs and is measured. The dimensions of the channel are 1 mm high, 3.18 mm wide and 5.2 mm long.

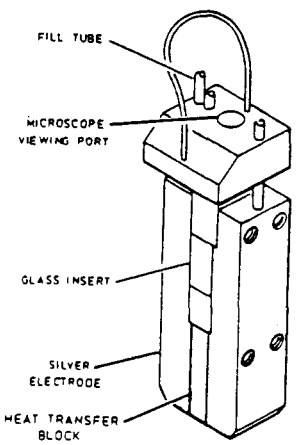

Figure A4.1 DELSA Sample Cell (Coulter, 1989)

The laser is a polarized 5 mW Helium-Neon Laser. The laser beam is split into 5 beams; a main beam and 4 reference beams. The intensity of the main beam is about 20 times greater than the reference beams. The beams intercept at the middle of the channel and the four reference beams go to four detectors. Each of the four detectors is a photo detector with a slow correlator so that the reference beam will be compared with the light reflected from the main beam by the particles in the sample channel. The beam size is about 0.05 mm high by 0.3 mm wide when it reaches the sample chamber channel.

An IBM PS2 computer is used to analyze the data from the photocorrelators and calculate the electrophoretic mobilities of the particles in the sample cell as described in the next section.

A microscope is mounted on the frame of the DELSA 440 so that the operator can look into the cell. This allows the operator to look for bubbles which might be in the cell and ensure that the laser beams are aligned so they cross in the middle of the cell.

A4.1.2 Laser Doppler Velocimetry

Laser Doppler Velocimetry is based on the Doppler effect where the frequency of a wave is altered when the source of the wave is moving. This happens in sound waves and light waves. In the case of light, the frequency of the light can be changed by bouncing the light off of a moving particle. The frequency shifts which occur in the DELSA electrophoresis are usually between 10 and 250 Hz.

When using laser light, which has a frequency of 1,000,000 Hz, a possible way to detect a shift of 10 Hz is to use the technique of light beating. Light beating is done by comparing the frequency of shifted and unshifted light waves. The two light waves interfere to produce a very low frequency oscillation superimposed on the high frequency light wave (as shown in Figure A4.2). This frequency caused by the two waves interfering is called the beat frequency (or the Doppler shift) and can be detected by a photo detector with a slow correlator.

Using Doppler theory, the beat frequency of the two waves can be converted into the velocity of the particle which reflected the light and caused it to shifted. In the DELSA 440 the two waves which are compared are the reference beam and light scattered from the main beam. There are four reference beams which require four correlators and give four values for the velocity of the particle.

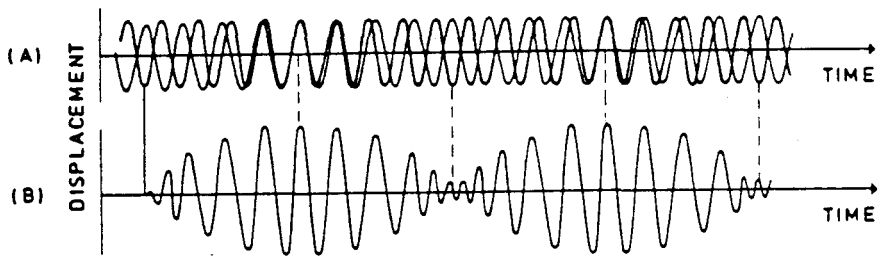

Figure A4.2 Beat frequency of two interfering light waves. The two waves in (A) interfere to give the oscillation shown in (B) (Coulter, 1989)

The DELSA 440 measure a correlation function which is fitted to a range of velocities which represents a range of particle velocities. Particles will have different velocities because of variations in the size and surface charge on the particle, Brownian motion and the position of the particle in the volume of intersection of the beams. A discussion of the interpretation of this distribution is contained in Data Analysis section of this appendix.

A4.1.3 Electrophoretic Mobility

Electrophoretic Mobilities can be calculated from the velocity measurements which were obtained by the Doppler shift measurements by applying the definition of electrophoresis. The electrophoretic mobility is defined as the terminal velocity of a particle moving as a result of an electric field acting upon the particle. The mobility is the terminal velocity divided by the electric field or:

$$\mu = V / E \qquad \text{(A4.1)}$$

where μ is the electrophoretic mobility, V is the terminal velocity (i.e.. the Doppler shift velocity) and E is the applied electric field. The electric field can be found by dividing the voltage applied to the cell by a cell constant.

A4.1.4 Electro-osmosis

Electro-osmosis is the flow of liquid adjacent to a charged surface caused by the application of an electric field. In the case of the DELSA apparatus, the charged surface is the quartz sides of the sample channel and the fluid is usually water with electrolyte ions. The quartz has a surface charge resulting from oxides on the surface of the quartz which causes a counter charge region to develop adjacent to the surface. When an electric field is applied, to perform electrophoresis, the charges move and cause a flow water next to the surface. In a closed cell the flow along the wall must be balanced by a flow back in the middle of the cell so a parabolic flow profile is developed (as shown in Figure A4.3).

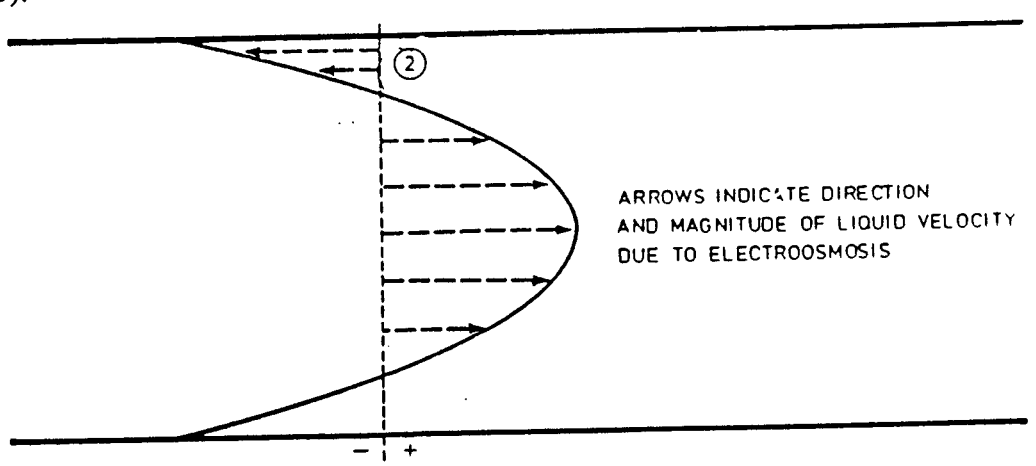

Figure A4.3 Electro-osmotic flow profile in a rectangular cell (Coulter, 1989)

The flow adjacent to the walls can be assumed to be exactly at the wall because the distance from the wall where the flow is maximum has been shown to be only 3/k where K is the inverse Debye Huckel length (Hunter,1981).

Assuming the flow was right next to the wall, Komataga solved the flow profile for a rectangular cell, neglecting end effects, to arrive at an equation for the velocity of the fluid as a function of the position and the height and the width of the cell. In electrophoresis experiments all measurements are made along the center width of the cell so the equation can be simplified so it is only a function of the vertical position. The simplified equation is (Hunter,1981)

$$U_{EO} = V_w - V_w \frac{3\,(1-y^2/h^2)}{2-384/\pi^5 K} \qquad \text{(A4.2)}$$

where U_{EO} is the velocity of the fluid do to electro-osmosis,

V_w is the velocity of the fluid at the wall,

y is the distance above or below the middle of the cell,

h is the distance from the middle to the wall and

K is the ratio of the width to the height of the cell.

In the DELSA cell h=0.5 mm K=3.18 and y can be found by subtracting the value for the position in the cell, from the micrometer by the value for the middle of the cell, that is,

$$y = y' - y_m, \qquad \text{(A4.3)}$$

where y' is the micrometer reading and y_m is the value for the middle of the cell.

The existence of electro-osmosis means that electrophoresis measurements cannot be made anywhere in the cell. There are two techniques that have been used, by researchers, to get meaningful data. One technique is to solve the Komataga equation for the position where the flow caused by electro-osmosis is zero and find the mobility at exactly this point. This position is called the stationary layer.

The position of the stationary layer can be found by setting U_{EO} to zero, in the Komataga equation (A4.2), giving,

$$y_0^2 = h^2 \ (1/3 + 384/3\pi^5 K) \qquad \text{(A4.4)}$$

For the DELSA cells h=0.5 mm and K=3.18 so the stationary layer can be found at ± 0.34 mm from the middle of the cell or at positions 16 and 84 on the micrometer.

Another technique is to find several mobilities at various positions across the cell and then fit these values to the komataga equation and solve for the mobility. The advantages and disadvantages of these two methods will be discussed in the Data Analysis section of this appendix.

A4.2 Experimental Procedure (Supplementary to Delsa Manual)

The Coulter Delsa 440 Manual contains an extensive description of the experimental procedures for the operation of the Delsa 440 Electrophoresis. However, some of the techniques described by the manual were expanded upon during the course of this thesis. These improvements include some tricks of sample preparation, some things to look for when running the machine to tell if there are any problems, and a new method for finding the stationary layer

A4.2.1 Sample Preparation

Sample preparation is one of the most time consuming operations involved in running the electrophoresis. It is difficult to prepare a sample with no air bubbles in the cell. Air bubbles can deflect the laser beams away from the detectors and can disturb the parabolic flow profile which should develop during electrophoresis. Bubbles can be prevented by applying a vacuum to the sample before it is inserted into the sample cell. This removes most of the dissolved air and greatly reduces the chance of bubbles developing in the middle of a set of measurements.

A4.2.2 Finding the Stationary Layer

The Coulter manual describes a technique for finding the stationary layer in the cell by observing the point where none of the laser light passes through the latex in the cell and setting this as the cell wall. By finding the wall on the top and bottom of the cell it is then easy to set the middle of the cell from which the stationary layers can be found.

The observation of the point where none the laser light is passing through the latex requires a visual judgement which is often difficult to make and becomes almost impossible when the sample in the cell is very dilute. As well, after making the visual judgement, the door to the sample chamber must be closed which sometimes jars the sample and upsets the setting on the micrometer.

The difficulties in finding the stationary layer can introduce severe errors in to the mobility measurements unless some improvements can be made. Two techniques have been developed to do this. The first involves taking measurements made at several places across the cell and fitting these to a parabola. Comparing the fitted parabola with the Komataga equation allows the calculation of both the electrophoretic mobility and the middle of the cell. This will be described in greater detail in the Data Analysis section of this appendix. Another new technique involves finding the stationary layer.

The new technique for finding the stationary layer is based on the observation that the edge of the crystal at the top and the bottom of the cell block some of the light from passing through. The edge of the cell can be detected then by watching for changes in the intensity of light which reaches the detectors. This can be done with the door closed and does not depend on the concentration of the latex in the cell.

To find the stationary layer place the sample cell firmly in the sample chamber, check for bubbles and then close the door. Select the Detector Levels screen and change the beam intensities until all detector levels are at maximum values (i.e. >12). Move the position of the cell up or down until the values drop from the maximum. Continue to move the cell until all levels have returned to the maximum except one. Position the cell

so that one angle is just off of the maximum value (around 12.0) and set this as a cell wall position. Repeat this procedure at the other wall. The middle of the cell is halfway between the two detected walls. Position the cell at the middle value and then set the micrometer to 50. The two stationary layers can be found by moving 34 micrometer units in either direction from the middle.

A4.2.3 Running Samples

After spending the time preparing a perfect sample it is important to get all the information you could possibly use out of each run. A few points which can help in the collection of reliable data are discussed in this section.

A4.2.3.1 Voltage Selection

An important parameter to set when running a sample is the voltage or current which will be applied across the cell. If the voltage is too high the sample may be damaged. Short runs at a test voltage before doing a full run can prevent damage to a sample. If the conductivity of the sample changes substantially between the beginning and the end of the run then the voltage or current is too high.

The voltage does not have to be the same at each position across the cell because both the particle velocity and the electro-osmotic flow are linear equations of voltage. If the voltage is varied the particle velocity and electro-osmotic flow will vary proportionally so the fraction of measured velocity over voltage will be a constant. The effect of voltage on the mobility was tested and some data was collected to prove that the mea-

sured mobility is not a function of the applied voltage. The data in Figure A4.4 shows that this assumption is valid for the Coulter Standard solution and for the NIPAM particles used in this thesis. Varying the voltage does not change the measured mobility so it is possible to select the voltage which will give the best results at each different cell position.

Voltage	7.5	15	22.5	34	Ave
a) Coulter Sample					
7	5.92	5.87	5.85	5.87	5.88
14	5.92	5.87	5.85	5.87	5.88
21	5.92	5.87	5.85	5.87	5.88
b) NIPAM Sample					
5	6.64	6.11	6.2	6.17	6.28
10	6.64	6.17	6.29	6.17	6.32
15	6.64	6.31	6.2	6.17	6.33
20	6.67	6.17	6.29	6.17	6.33

Figure A4.4 Mobility data showing no dependence on the applied voltage for a Coulter standard sample and a poly (NIPAM) sample.

If you cannot get a high enough frequency shift with a reasonable voltage then try moving the cell to a new position. Often the mobility at the stationary layer is too low to be detected directly, but by using a fit to a parabola, as described in the Data Analysis section of this Appendix, it is possible to avoid areas where the mobility is hard to measure and therefore avoid damaging the sample.

Electrophoresis measurements made at high voltages may be affected Joule heating effects. Joule heating is caused by the energy absorbed by a fluid when it is sheared. The movement of the fluid in the cell because of electro-osmosis can sometimes cause enough Joule heating to raise the temperature of the cell and change the conditions of the measurement. The time off value can be set higher than the time on value to avoid over heating the sample. This will allow the fluid in the cell to return to the set temperature before another measurement is made.

Ware and Flygare (1972) found that an off to on ratio of 10 to 1 eliminated Joule Heating when voltages of 150 V were used but it was found that for low voltages (<20 V) a 1 to 1 ratio was sufficient. Ware and Flygare also found that the minimum on time required was around 0.12sec which allowed the system to reach steady state.

A4.3 Data analysis

The raw data from the measurements of the electrophoretic mobility are of little value unless they are understood and corrected for errors in finding the middle of the cell and imperfect tuning. This section discusses the techniques of data analysis which were used to get reproducible and meaningful results.

A4.3.1 Distribution Analysis

The result from an experimental run is a distribution of frequencies or mobilities. The distribution is a result of Brownian motion, variations in the particles and a range of positions within the beam intersection volume. The DELSA provides two choices for the analysis of the average of the distribution; the mode and the mean of the distribution

The mode is the point on the distribution with the highest frequency of occurrence or the peak of the distribution. Alternatively, the mean is the frequency weighted average of the entire distribution. Both of these choices have advantages and disadvantages which will determine which of the two is used to analyse the results.

The advantage of the mean is that the results also indicate the standard deviation and the skewness of the distribution which provides more information. The disadvantage is that it is difficult to define which parts of the distribution will be included in the analysis.

The distribution often has small side peaks (shown in figure A4.5) which are a not real but are a result of imperfect heterodyne ratios. These side peaks are difficult to accu-

rately exclude from the distribution and if included will shift the mean of the distribution. The mean of the distribution is only accurate when the distribution is perfectly smooth which very rarely occurs.

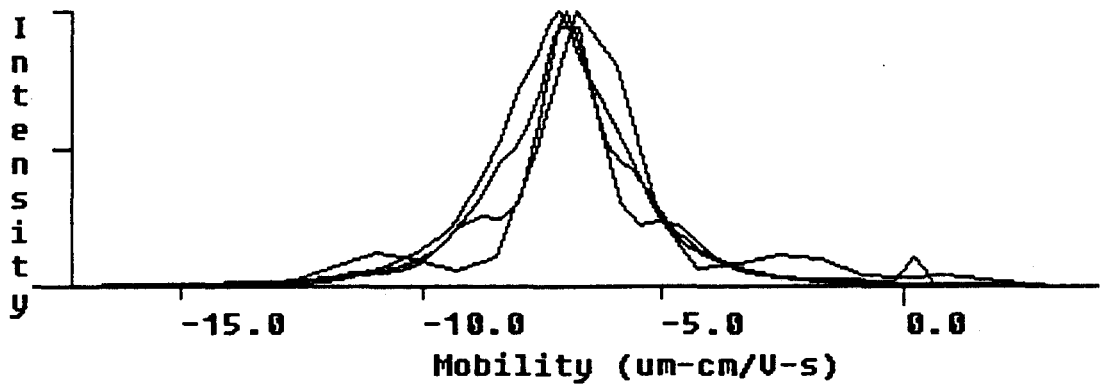

Figure 4.5 A series of mobility curves showing the side peaks which exist and make the evaluation of the mean mobility difficult to determine

The advantage to the selection of the mode is that it is easy to find and does not require the careful selection of the region to be analyzed. The disadvantages are that no data can be gathered about the deviation or skew of the distribution and some distributions have two peaks. Distributions which have two peaks (as shown in Figure A4.6) can not be accurately analyzed used the mode analysis.

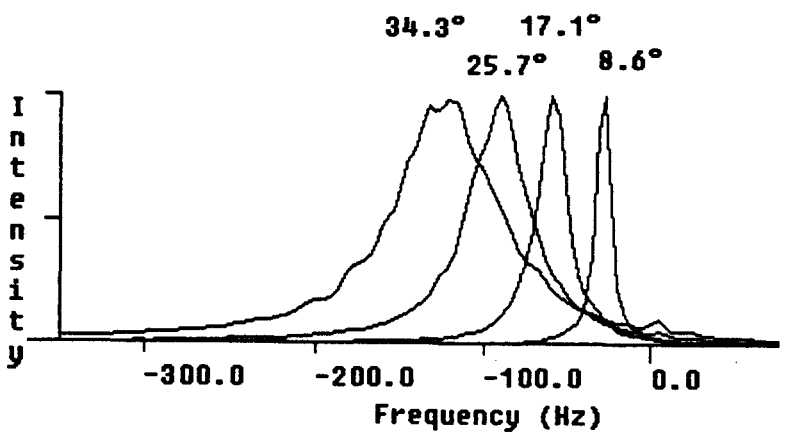

Figure A4.6 Electrophoresis frequency shift result showing double peak on the 34.3° angle detector.

A4.3.2 Correcting for Electro-osmotic Flow

Electro-osmosis causes a parabolic flow profile to develop in the cell which must be accounted for when making mobility measurements. As mentioned previously, there are two ways of dealing with this problem. The first is to find the position on the parabola where the electro-osmotic flow is zero and the second is to find the mobility at several different points across the cell and fit them to a parabolic curve.

Using the zero electro-osmotic flow position, which is called the stationary layer, can be done quickly but the results are unreliable. To find the stationary layer the operator must first find both of the cell walls and then position the cell accordingly. In the DELSA system where the cell is only one millimeter high the stationary layer is very difficult to find accurately and, since the flow profile at the mobility layer is quite steep, the mobility measurements are susceptible to error.

The measurement procedure can be improved by measuring the mobility at the other stationary layer and averaging the two. The fit to parabola method however requires only a few more measurements and gives much better accuracy.

The fit to parabola method requires several measurements across the cell. A set of positions which could be chosen would be the two stationary layers, the middle of the cell and two other points which were on either side of the middle of the cell. A plot of these points (Figure A4.7) shows the parabolic shape of the mobility measurements. In order to find the true mobility or the mobility at the actual stationary layer it is necessary to fit these points to a parabolic curve. This can be done by using a linearized parabolic

curve equation and fit the points to a straight line (as shown in Figure A4.7)

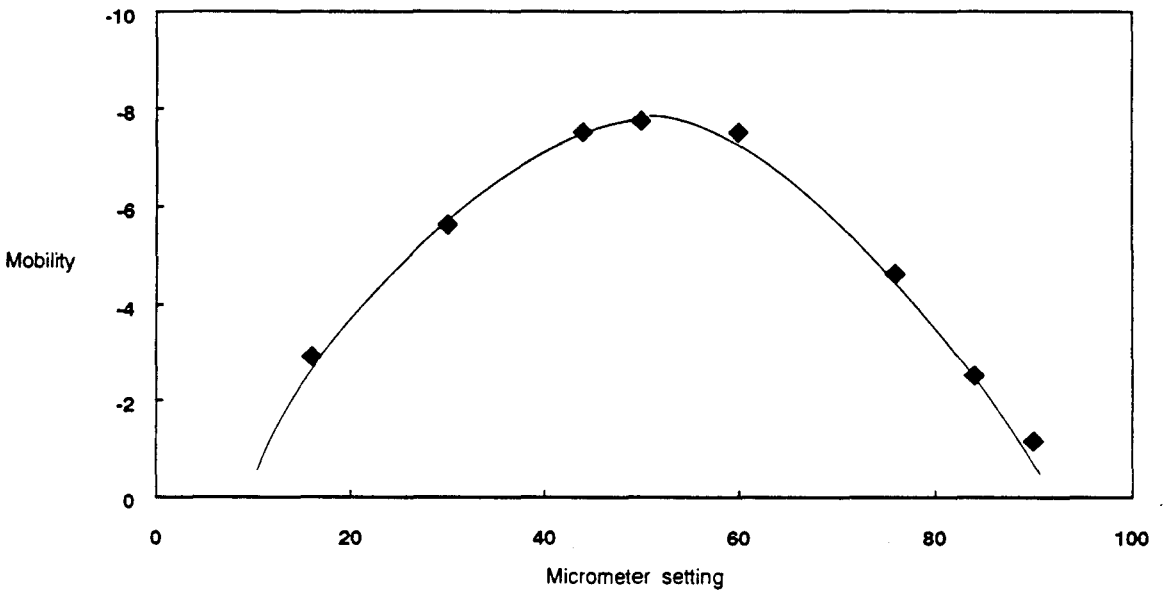

Figure A4.7 Parabolic flow profile as shown by mobility measurements across the sample cell

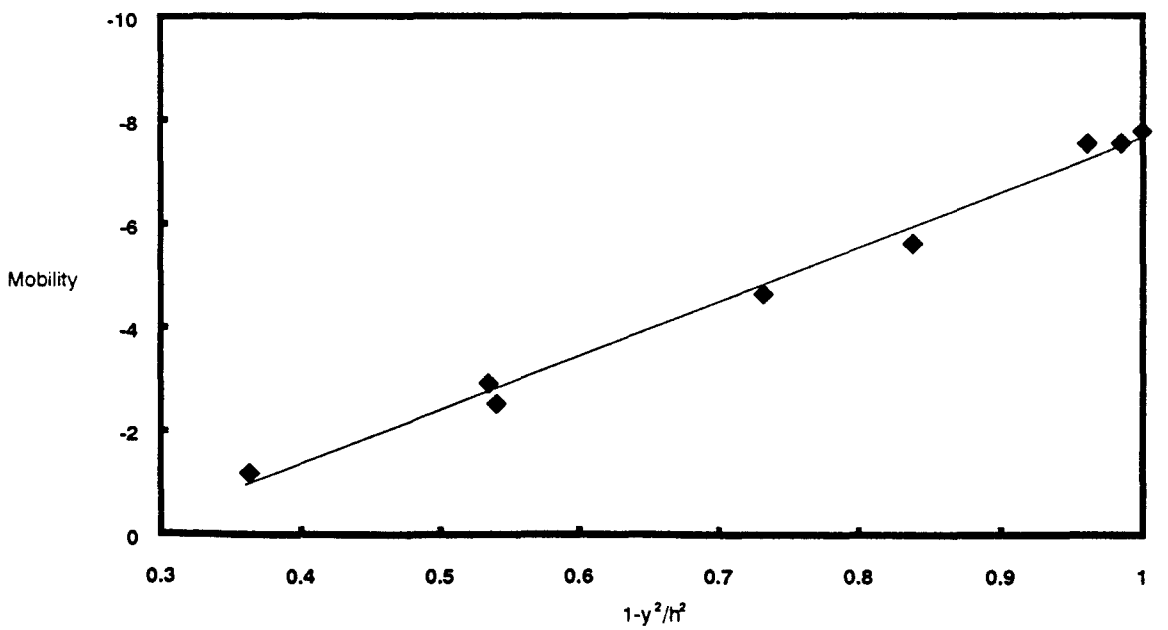

Figure A4.8 Linearized parabolic flow profile

The equation used to fit the data points and find the true mobility is based on the Komataga equation. The particle velocity measured at any point is the summation of the electro-osmotic fluid velocity and the particle mobility or,

$$U_{meas} = U_{EO} + \mu \qquad \text{(A4.5)}$$

where U_{meas} is the measured velocity of the particles,

U_{EO} is the electro-osmosis fluid velocity and

μ is the actual mobility of the particles.

Substituting the Komataga equation (A4.2) for U_{EO} gives,

$$U_{meas} = \mu + V_w + \frac{3(1-y^2/h^2)}{2 - 384/\pi^5 K} V_w \qquad \text{(A4.6)}$$

The equation can be linearized by replacing $1-y^2/h^2$ with x so that the equation is now linear,

$$U_{meas} = \mu + V_w + \frac{3 V_w}{2 - 384/\pi^5 K} \qquad \text{(A4.7)}$$

with a slope of $3Vw / (2-384/\pi^5K)$ and a y-intercept of $\mu + Vw$.

A line fitting function like least squares can be used to fit the data to a line and solve for the wall velocity and the true particle mobility.

The advantages to this technique are numerous. The mobility can be found accurately, the middle of the cell does not have to be found accurately and it is easy to spot errors in the positioning of the cell by looking at the plot of the parabola.

Another important advantage is that it is possible to find mobilities which are two low to be measured at the stationary layers by extrapolating a parabola which is found near the middle of the cell. When the mobility is very low the voltage required to get a reasonable frequency shift at the stationary layer is very high. To avoid high voltages no measurements are made at the stationary layer. Instead measurements are made as near to the stationary layer as possible and at several other points so that a parabola can be fit. The equation of the linearized parabola which is found from these values is extrapolated to the stationary layer so that the true mobility can be found (see Figure A4.9 and A4.10).

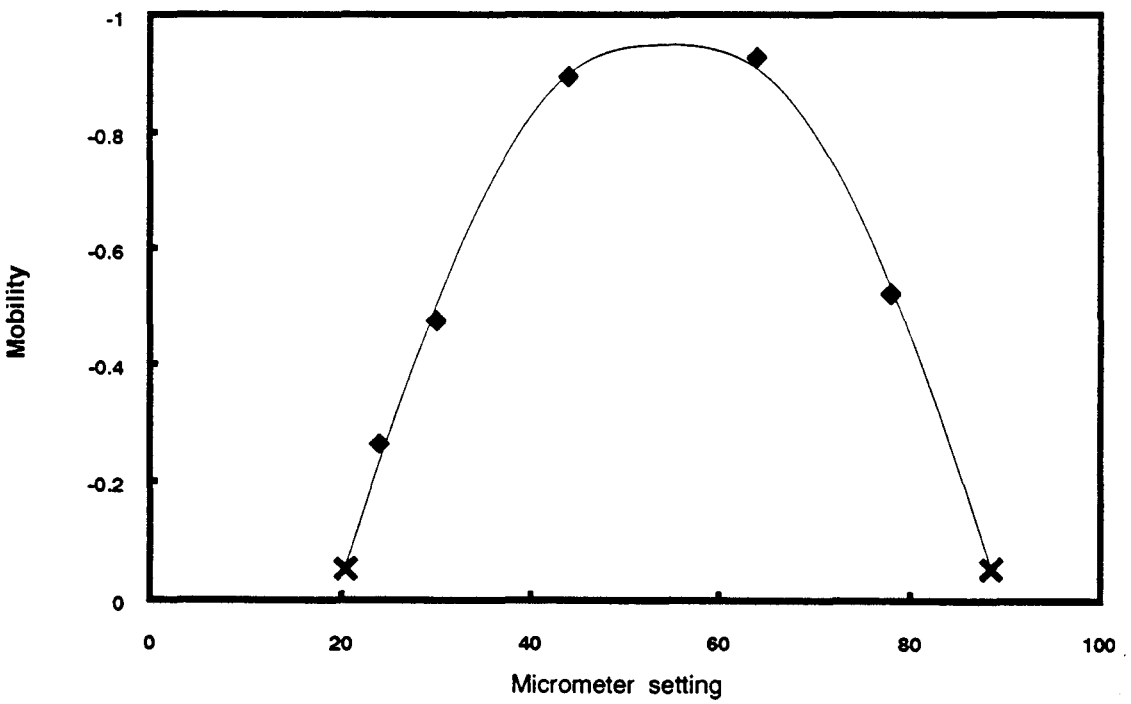

Figure 4.9 The mobility of a low mobility sample found by extrapolating the parabolic profile to the stationary layer (marked by an X)

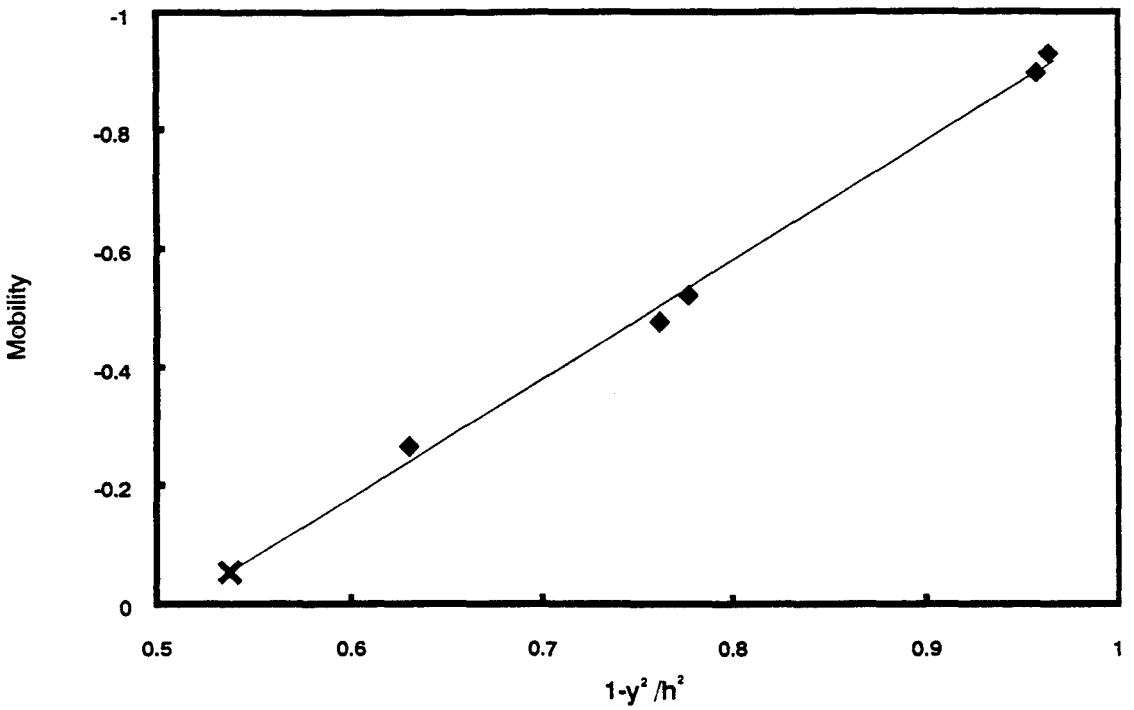

Figure 4.10 A linearized parabola showing the extrapolation used to find the mobility of a low mobility sample.

A4.3.3 Correction for Imperfect Tuning

The DELSA will sometimes show a non-zero frequency shift when the applied voltage is zero. This is generally attributed to residual flow in the cell caused by either temperature gradients or evaporation from the filling and emptying tubes of the cell.

If these explanations were true then it would be expected that the frequency shifts in the positive and negative directions would be equal in magnitude and opposite in sign. The shift however is always of the same sign in both directions. This suggests a problem with the tuning of the laser beams.

Measurements of the mobility taken with applied voltage can be effected by the imperfect tuning and must be corrected. The measured frequency shift, with an applied voltage, will have an error equal to the zero voltage frequency shift. The corrected frequency shift will be the measured minus the zero voltage frequency shift.

The fraction of error in the frequency shift is proportional to the error in the mobility. The mobility can be corrected by multiplying the measured mobility by the ratio of the corrected frequency shift over the measured frequency shift,

$$\mu' = \mu\,(\lambda-\lambda_o)/\lambda \qquad \text{(A4.8)}$$

where μ' is the corrected mobility,

μ is the measured mobility,

λ is the measured frequency shift and

λ_o is the zero voltage frequency shift.

The mobility data corrected for the zero voltage frequency shift are more accurate and more reliable than the uncorrected data.

A4.3.4 Correction for Error in Finding the Middle of the Cell

Finding the middle of the cell is extremely difficult and is prone to error. Given that the error in finding the middle of the cell is inherent, it is necessary to find a way to correct for this error.

The fit to parabola method which uses a least squares fit to a straight line is ideally suited to correction. The value for the micrometer value for the middle of the cell can be used as a variable which can be changed to improve the fit of a straight line to the data. The best fit line then is the line which minimizes the deviation between the experimental data and the least squares approximation.

The value for the middle of the cell is used to convert micrometer readings into the proper y values for the parabola equation. The conversion is,

$$y = y' - y_m \qquad \text{(A4.3)}$$

where y is the y value for the parabola equation, y' is the micrometer reading and y_m is the value for the center of the cell. When trying to find the best line it is reasonable to use a guess of 50 first since this would be correct if the middle of the cell had been found correctly.

To find the value for the middle of the cell which gives the least deviation it is necessary to define an appropriate deviation function. The most common function used to express the deviation in a linear fit is the coefficient of determination (r^2).

The value of r^2 in this case represents the fraction of the deviation in the mobility values which can be accounted for by the linear relationship between the linearized parabola and the mobility. For instance, a value of r^2=0.99 means that 99% of the deviation in the mobility values can be accounted for by the linear fit.

The best fit line can be found by maximizing the value of r^2. The values of r^2 can range from 0 to 1 where a value of 0 means that no linear fit exists and a value of 1 that the linear fit is perfect. Linear fits of mobility that had r^2 values less than 0.98 were considered to have too much error and were re-evaluated or discarded.

Experiments with r^2 values less than 0.98 were usually the result of uncorrected zero voltage frequency shifts, bubbles or movement of the sample cell in the sample chamber.

A4.3.5 Averaging the Mobilities at the Four Angles

The DELSA has four detection angles which give four values for the electrophoretic mobility. In the ideal case, these are very close in value or can be corrected, as discussed above, to become very close in value. When the four angles give similar values, it is appropriate to take an average of the four values as a good value for the mobility. Sometimes however, the values at one or two angles are significantly different from the rest.

These variations usually occur at the highest or the lowest angle for explainable reasons. At the low angle the data is often inaccurate because of relatively large bin sizes. For instance, a 10 Hz frequency shift is considered adequate to get reliable results but if the experiment was done with a 1000 Hz frequency range the bin size will be 3.9 Hz which would make the error in the 10 Hz frequency shift about 20%. The mobility value for the lowest angle would have a large error if the error at each point on the

parabola was 20% so the value can be discarded and an average of the remaining three angles used as a good value.

At high angles the frequency shift distribution can have a double peak, as shown previously in Figure A4.5, which can introduce error to some of the points and to the mobility value for the highest angle.

The results at each point should be examined carefully so that errors at each angle can be minimized. The mobility data can then be accepted with confidence or discarded if appropriate.